Physics
University of Pisa

Master Thesis

Quantum capacity analysis of 4-dimensional Multi-level Amplitude Damping channels

Explanatory subtitle

by
Marco Cocciaretto
547875

Supervisor: Vittorio Giovannetti
CdS Tutor: Davide Rossini
Date: September, 2023

Abstract

Quantum Information Theory (QIT) is a relatively new field of physics that is attracting a growing number of researchers. Although some elements of QIT can be found at the dawn of Quantum Mechanics (e.g. the EPR paradox), its first formal definition dates back to the 1960's[Gor62] (Bell published his paper on the EPR paradox in 1964[Bel64]).

The new framework provided by the QIT allowed for the study of open systems, i.e. systems subject to external noise; this is accomplished by defining any quantum process as a **L**inear, **C**ompletely **P**ositive and **T**race-preserving (LCPT) map, which interpret the set of initial density matrices as input and output new density matrices in a (possibly) different Hilbert space. This paved the way for an information theoretic approach to the study of quantum processes relevant to Quantum Computation and Quantum Communication, in the same way Shannon's noisy channel theorem did for classical communication.

The question then becomes, in this context, what quantity can we interpret as "information"? And how well is this information preserved during the quantum process? In other words, how well can we store and reliably transmit information through a given channel? It turns out that, in the quantum case, the amount of "stored information" of a system is given by the Von Neumann entropy, while there are a number of quantities called "capacities" that describe the amount of transmittable information through a given channel based on the nature of the information to be transmitted and the availability of additional resources (e.g. classical communication lines, entanglement...). This thesis work focuses on the study of some of these capacities, with a particular focus on quantum capacity and 2-way quantum capacity, for a specific family of channels, called Multilevel Amplitude Damping (MAD) channels.

MAD channels are the d-dimensional extension of the well understood 2-dimensional case of Amplitude Damping Channels. The foundations for how to treat these kind of channels were already laid out in an earlier work by V. Giovannetti and S. Chessa[CG21a], which explored the channels in the case of $d = 3$.

The quantum capacity is generally not computable, as its underlying quantity (the coherent information) is not subadditive when one considers multiple uses of a channel. The only cases in which the quantum capacity is computable correspond to degradable (i.e. there exists a LCPT map that connects the output state of the system to the output state of the environment, which takes on the role of the induced noise) and anti-degradable (i.e. there exists a LCPT map that connects the output state of the environment to the output state of the system; in this case the quantum capacity is 0) channels. When neither of these conditions is satisfied, it is usually only possible to set upper and lower bounds on the quantum capacity.

In [CG21a] it has been shown that it is possible to find the value for the quantum

capacity of 3-dimensional MAD channels even in regions where those channels are neither degradable nor anti-degradable. This was accomplished by employing the pipeline inequalities, which led to the derivation of some monotonicity properties for the capacity that allowed to extend the values of the capacity found at the border of the degradability regions to the outside of these regions. Expanding upon this work, some general results for d-dimensional MAD channels were found (i.e. composition, monotonicity properties, inverse maps, degradability conditions), which enabled a generalization of the technique used to find the quantum capacity in non-degradability zones in [CG21a]. This paved the way for the numerical evaluation of the quantum capacity for various configurations of 4-dimensional MAD's, again, even where those channels are not degradable.

The 2-way quantum capacity of 3-dimensional MAD channels was also studied, as the literature was lacking in that regard, and upper and lower bounds (which are always computable) were found.

The results of the thesis are to be added in the context of those related to the computation of the quantum capacity for qudit channels (which suggest that these channels could be more convenient with respect to their qubit counterparts) and to those related to the limits of repeater-less quantum communication. The techniques illustrated in the thesis can be ideally expanded to bigger dimension, the limit being the computational power of the machine used to arrive at the values of the capacities.

Contents

Nomenclature

Abbreviations

Abbreviation	Definition
QIT	Quantum Information Theory
QCT	Quantum Communication Theory
LCPT	Linear, Completely Positive, Trace-preserving
ADC	Amplitude Damping Channel
MAD	Multi-level Amplitude Damping

Variable Names

Symbol	Definition	Unit
α	greek alpha	[N]
β	greek beta	[J]

1

Introduction

2

Theory of Quantum Information and Communication

In this chapter, the reader will be presented with all the tools necessary to understand this thesis work. The theories that encompass these tools are called Quantum Information Theory (QIT) are Quantum Communication Theory (QCT). The strength of these theories lies in the fact that they provide a framework that makes it possible to study the behavior of *open systems*, which will be defined in the following section. The reason behind the necessity of a coherent structure describing open system is a practical one: in any real world scenario, physicists will find themselves having to deal with *noise*, which is something that only an open system can take into account. The work of Shannon [Sha48] taught the scientific community how information is transmitted through a classical, noisy communication line. Quantum Information Theory allows for the study of *quantum noise*, which in turns paves the way for the development of, to name a few, Quantum Computers (whose component are very susceptible to external perturbations). Something something large number prime factoring something something quantum teleportation

2.1 Open Systems

Usually, in quantum mechanics, the time evolution of the system in a state can be summarized by defining a unitary operator, dependent on the Hamiltonian of the system. This is done through the Schrödinger equation:

$$i\hbar\frac{\partial}{\partial t}\left|\psi(t)\right\rangle = H\left|\psi(t)\right\rangle, \tag{2.1.1}$$

where $\left|\psi(t)\right\rangle$ is the state of the system at time t and H is the Hamiltonian operator. Solving (2.1.1) yields:

$$\left|\psi(t')\right\rangle = \exp\left[iH(t'-t)/\hbar\right]\left|\psi(t)\right\rangle \tag{2.1.2}$$

This picture only works for time-independent Hamiltonians[1] and for *closed systems*, i.e. systems whose interactions are confined within said systems. This is not generally the case in a real-world setting, as physicists often have to deal with noise, which can be represented as an interaction of the *laboratory system* (i.e. the system upon which one is able to make measurements) with an external system, usually called *environment*. Before defining a framework capable of describing this scenario, a precise definition of *quantum state* is needed. The most generic quantum state of a system $\mathcal{H}$ takes the form of a *density matrix operator* ρ, which satisfies the following properties:

- ρ is a hermitian operator, $\rho^\dagger = \rho$.
- $\operatorname{tr}\rho = 1$.
- $\operatorname{tr}\rho^2 \leq 1$; if $\operatorname{tr}\rho^2 = 1$ then the state is called a *pure state*, i.e. $\exists\,|\psi\rangle \in \mathcal{H} : \rho = |\psi\rangle\langle\psi|$. A state that is not pure is called *mixed state*.
- ρ is positive-semidefinite, $\rho \geq 0$.

The set of all the elements that satisfy the properties above is denoted as $\sigma(\mathcal{H})$. In order to characterize the interaction of a system $\mathcal{H}_S$ with an environment $\mathcal{H}_E$, one needs to consider *joint states* $\rho_{SE} \in \sigma(\mathcal{H}_S \otimes \mathcal{H}_E)$, which represent the total states of the system laboratory-environment. In general, given a joint state $\rho_{AB} \in \sigma(\mathcal{H}_A \otimes \mathcal{H}_B)$, one could obtain the *reduced* density matrices, representing the states of the systems $\mathcal{H}_A$ and $\mathcal{H}_B$ through the use of the *partial trace* operation, defined as:

$$\begin{aligned} \rho_B &= \operatorname{tr}_A \rho_{AB} \equiv \sum_i {}_A\langle\phi_i|\rho_{AB}\,|\phi_i\rangle_A \\ \rho_A &= \operatorname{tr}_B \rho_{AB} \equiv \sum_i {}_B\langle\psi_i|\rho_{AB}\,|\psi_i\rangle_B \end{aligned} \tag{2.1.3}$$

where $\{|\phi_i\rangle_A\}_i$ and $\{|\psi_i\rangle_B\}_i$ are, respectively, bases of $\mathcal{H}_A$ and $\mathcal{H}_B$. Then, let $\rho_S \in \sigma(\mathcal{H}_S)$ and let the state of the environment be a pure state[2] which will be denoted as $\tau_E = |0\rangle_E\langle 0| \in \sigma(\mathcal{H}_E)$, then the state of the composite system $\mathcal{H}_S \otimes \mathcal{H}_E$ is the tensor product[3]:

$$\rho_{SE} \equiv \rho_S \otimes |0\rangle_E\langle 0| \in \sigma(\mathcal{H}_S \otimes \mathcal{H}_E)\,. \tag{2.1.4}$$

In section 2.3, the mechanism behind the evolution of ρ_S, in the setting illustrated above, will be explained.

[1] A solution for time-dependent Hamiltonians (which might not commute between themselves at different times) exists and is called *Dyson series*, see [Dys49]

[2] This is because, since the environment represents anything that is external to the system A, even if τ_E was, in fact, a mixed state, it could always be *purified*, see 2.2

[3] In order to lighten the notation, when possible, the symbol $\otimes$ of tensor product will usually be omitted, as indexes referring to specific quantum systems make it redundant.

2.2 Composite quantum states

Before moving on, it might be useful to label composite quantum states in a more precise way. Given a joint system $\mathcal{H}_S \otimes \mathcal{H}_R$, its quantum states ρ_{SR} can be classified in one of the three following categories:

- *Factorized states* present the form:

$$\rho_{SR} = \rho_S \tau_R, \tag{2.2.1}$$

- *Separable states* present the form:

$$\rho_{SR} = \sum_i p_i \rho_S^{(i)} \tau_R^{(i)}, \tag{2.2.2}$$

  where $\{p_i\}_i$ forms a probability distribution, $\sum_i p_i = 1$. Separable states are convex combination of factorized states; furthermore, the convex combination of separable states is still a separable state. Note that (2.2.2) reduces to (2.2.1) if $p_i = \delta_{i,i_0}$

- *Non separable (entangled) states* are all the joint states that do not satisfy (2.2.2)

Purification

Let ρ_S be a state in $\mathcal{H}_S$, suppose that ρ_S is a mixed state and let $\mathcal{H}_R$ be another system, called, in this case, *auxiliary* system. Through the *purification* process, it is **always** possible to build a composite state $\rho_{SR} \in \sigma(\mathcal{H}_S \otimes \mathcal{H}_R)$, $\mathrm{tr}_R\, \rho_{SR} = \rho_S$ such that ρ_{SR} is a pure state. In fact, in its diagonal basis $\{|\psi_i\rangle_S\}_i$, ρ_S can be written as:

$$\rho_S = \sum_i p_i |\psi_i\rangle_S \langle\psi_i| \tag{2.2.3}$$

where p_{ii} forms a probability distribution. Then, fixing $\dim \mathcal{H}_R = \dim \mathcal{H}_S$ and choosing a basis $\{|i\rangle_R\}_i$ for $\mathcal{H}_R$, one could build the pure state:

$$\begin{aligned} |\psi_i\rangle_{SR} &\equiv \sum_i \sqrt{p_i} |\psi_i\rangle_S |i\rangle_R \\ \rho_{SR} &= |\psi_i\rangle_{SR} \langle\psi_i| \end{aligned} \tag{2.2.4}$$

which clearly satisfies $\mathrm{tr}_R\, \rho_{SR} = \rho_R$.

2.3 Stinespring Dilation

Since the composite system $\mathcal{H}_S \otimes \mathcal{H}_E$ is a closed system, its state in (2.1.4) will evolve following a unitary operator $U_{SE} : \mathcal{H}_S \otimes \mathcal{H}_E \mapsto \mathcal{H}_S \otimes \mathcal{H}_E$, which acts on density matrices as:

$$\rho_{SE} \mapsto U_{SE} (\rho_S |0\rangle_E \langle 0|) U_{SE}^\dagger. \tag{2.3.1}$$

Then, combining (2.3.1) with (2.1.3), one could find the evolved state of the system S by defining a *superoperator* (i.e. an object that maps linear operators into linear operators) Φ such that:

$$\rho_S \mapsto \Phi(\rho_S) = \mathrm{tr}_E \left[U_{SE} (\rho_S |0\rangle_E \langle 0|) U_{SE}^\dagger \right]. \tag{2.3.2}$$

This equation defines a very specific family of maps: in fact any map Φ which can be cast in the form of (2.3.4) needs to satisfy the following properties:

- Φ is **L**inear,
- Φ is **C**ompletely **P**ositive, meaning that its Choi matrix (see **??**) is positive [Cho75],
- Φ is **T**race preserving, meaning that $\mathrm{tr}\,\theta = \mathrm{tr}\,\Phi(\theta)$ for all θ.

The maps satisfying these properties are named through the acronym LCPT maps, or, in the context of QIT, simply *quantum channels*.

One could also consider quantum channels whose input and output systems are different from each other. In this case, an input state $\rho_A \in \sigma(\mathcal{H}_A)$ is sent into an output state $\Phi(\rho_A) \in \sigma(\mathcal{H}_B)$. The channel

$$\Phi : \sigma(\mathcal{H}_A) \mapsto \sigma(\mathcal{H}_B) \tag{2.3.3}$$

can be defined by introducing an isometry $U_{BE\leftarrow AE}$, so that:

$$\rho_A \mapsto \Phi(\rho_A) = \mathrm{tr}_E \left[U_{BE\leftarrow AE} (\rho_A |0\rangle_E \langle 0|) U_{BE\leftarrow AE}^\dagger \right]. \tag{2.3.4}$$

In general, the map $\rho_A \mapsto U_{BE\leftarrow AE} (\rho_A |0\rangle_E \langle 0|) U_{BE\leftarrow AE}^\dagger$ is called *Stinespring dilation* [Sti55], while the map in (2.3.4) is the *Stinespring representation* of the quantum channel Φ; in fact, as will be explained in 2.4, a given LCPT map admits different but equivalent representations.

2.4 Channel representations

The Stinespring representation is not the only possible representation of quantum channels. In fact, it can be shown that there exist different representations equivalent to each other; the most important ones are reported below

2.4.a Stinespring representation

As seen in 2.3, the Stinespring dilation $\mathfrak{U}_{S\mapsto SE}$:

$$\begin{gathered} \mathfrak{U}_{S\mapsto SE}(\bullet) \equiv U_{S\mapsto SE} \bullet U_{S\mapsto SE}^\dagger \\ U_{S\mapsto SE} \equiv U_{SE} |0\rangle_E \\ \rho_S \xmapsto{\mathfrak{U}_{S\mapsto SE}} U_{SE} (\rho_S |0\rangle_E \langle 0|) U_{SE}^\dagger \end{gathered} \tag{2.4.1}$$

is an isometry that maps an input state in $\sigma(\mathcal{H}_S)$ onto a state in $\sigma(\mathcal{H}_S \otimes \mathcal{H}_E)$; tracing this *dilated* state over the environment E returns the output state $\Phi(\rho_S)$ (2.3.4). Note that the input and output system of the quantum channel do not need to coincide. This can be achieved by replacing the unitary U_{SE} with an isometry $U_{BE\leftarrow AE}$. This leads to a more general form of (2.4.1).

$$\begin{gathered} \mathfrak{U}_{A\mapsto BE}(\bullet) \equiv U_{BE\leftarrow A} \bullet U_{BE\leftarrow A}^{\dagger} \\ U_{BE\leftarrow A} \equiv U_{BE\leftarrow AE} |0\rangle_E \\ \rho_A \xmapsto{\mathfrak{U}_{A\mapsto BE}} U_{BE\leftarrow AE} (\rho_A |0\rangle_E \langle 0|) U_{BE\leftarrow AE}^{\dagger} \end{gathered} \tag{2.4.2}$$

2.4.b Kraus Representation

The Kraus representation is characterized by a set of operators $\mathcal{K} = \{K_i\}_i$ on $\mathcal{H}$ such that:

$$\sum_i K_i^{\dagger} K_i = \mathbb{1} \tag{2.4.3}$$

where $\mathbb{1}$ is the identity operator on $\mathcal{H}$. The set $\mathcal{K}$ describes a unique quantum channel Φ, defined by:

$$\Phi(\rho) = \sum_i K_i \rho K_i^{\dagger} \tag{2.4.4}$$

The set $\mathcal{K}$ is called *Kraus set*, while the K_i's are called *Kraus operators*. Note that unitary transformations are a particular class of quantum channels, as given the unitary operator U, one could build the trivial Kraus set $\mathcal{K} = \{U\}$ which satisfies (2.4.3) and the corresponding unitary transformation is given in the Kraus representation, $\rho \mapsto U\rho U^{\dagger}$.

It is possible, given a Stinespring representation of a channel, to derive (one of) its Kraus representations, in fact from (2.3.4):

$$\Phi(\rho_S) = \mathrm{tr}_E \left[U_{SE} (\rho_S |0\rangle_E \langle 0|) U_{SE}^{\dagger} \right] = \sum_l {}_E\langle l| U_{SE} |0\rangle_E \rho_S {}_E\langle 0| U_{SE}^{\dagger} |l\rangle_E . \tag{2.4.5}$$

Then, one could define:

$$K_i \equiv {}_E\langle i| U_{SE} |0\rangle_E , \tag{2.4.6}$$

which is an operator acting on $\mathcal{H}_S$ and that clearly satisfies (2.4.3), so that (2.4.4) is obtained. Conversely, one could obtain the Stinespring representation from a Kraus set by defining:

$$U_{SE} \equiv \sum_i K_i |i\rangle_E \langle 0| \tag{2.4.7}$$

Equivalence of Kraus representations

While a certain $\mathcal{K}$ identifies a specific Φ, given a channel Φ one may find different Kraus sets associated with it. It is then reasonable to ask under which condition two Kraus

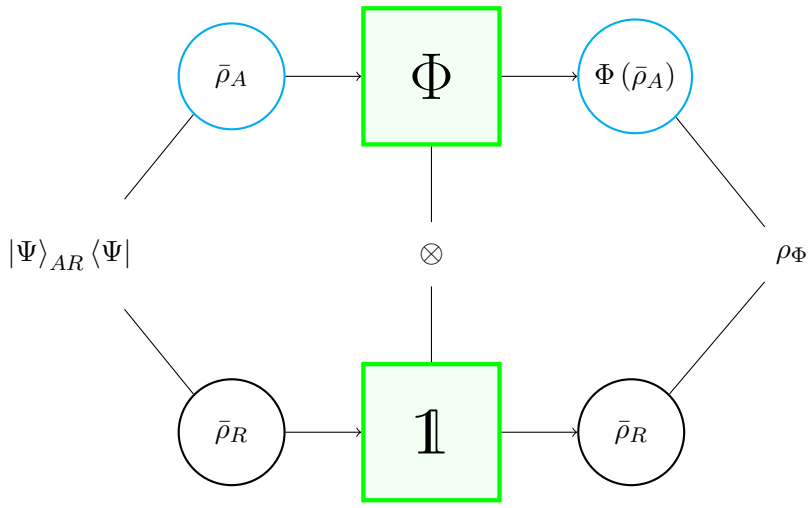

Figure 2.4.1: The Choi state ρ_Φ for a channel Φ can be built using the scheme described in this figure

sets represent the same quantum channel. The answer is that, given the Kraus sets $\mathcal{K} = \{K_i\}_i$ and $\mathcal{K}' = \{K'_i\}_i$, they represent the same channel if and only if:

$$K'_i = \sum_j \mathcal{U}_{ij} K_j, \tag{2.4.8}$$

where the $\mathcal{U}_{ij}$ are the matrix elements of an isometry and they satisfy the conditions:

$$\sum_k \mathcal{U}_{ik}\mathcal{U}^*_{jk} = \sum_k \mathcal{U}_{ki}\mathcal{U}^*_{kj} = \delta_{ij}. \tag{2.4.9}$$

TODO controlla indici.

2.4.c Choi-Jamiołkowski representation

The Choi-Jamiołkowski isomporphism [Cho75], [Jam72] introduces a one-to-one mapping between a channel and a specific density matrix. Consider the channel Φ acting on the system $\mathcal{H}_A$ of dimension d and a reference system $\mathcal{H}_R$; given the completely chaotic state $\bar{\rho}_A$:

$$\bar{\rho}_A \equiv \frac{1}{d}\sum_i |i\rangle\langle i|, \tag{2.4.10}$$

it can be purified using the reference system R, leading to the maximally entangled state $|\Psi\rangle_{AR}$:

$$|\Psi\rangle_{AR} = \frac{1}{\sqrt{d}}\sum_i |i\rangle_A |i\rangle_R. \tag{2.4.11}$$

If the state in system A is sent through the channel Φ the corresponding state in AR is sent through $\Phi \otimes \mathbb{1}_R$; if the maximally entangled state in (2.4.11) is sent through

$\Phi \otimes \mathbb{1}_R$, the output of this channel is called *Choi state* of the channel:

$$\begin{aligned} &\rho_\Phi \quad \text{Choi state} \\ &\rho_\Phi \equiv [\Phi \otimes \mathbb{1}_R] \left(|\Psi\rangle_{AR} \langle\Psi| \right) \end{aligned} \tag{2.4.12}$$

Figure 2.4.1 provides a visual depiction of Choi states. It is possible to prove (see **??**) that:

$$\begin{aligned} \Phi \left(|\psi\rangle_A \langle\psi| \right) &= d \, {}_R\langle\psi^*| \rho_\Phi |\psi^*\rangle_R \\ &= d \, \mathrm{tr}_R \left(|\psi\rangle_R \langle\psi| \left(\rho_\Phi\right)^{T_A} \right) \end{aligned} \tag{2.4.13}$$

where

$$\begin{aligned} |\psi\rangle &= \sum_{i=0}^{d-1} \alpha_i |i\rangle \\ \Rightarrow |\psi^*\rangle &= \sum_{i=0}^{d-1} \alpha_i^* |i\rangle \, . \end{aligned} \tag{2.4.14}$$

and the operation of *partial transpose* has been introduced:

$$\begin{aligned} \theta_{AR} &= \sum_{ijmn} \theta_{ijmn} |i\rangle_A \langle j| \ |m\rangle_R \langle n| \\ \Rightarrow \left(\theta_{AR}\right)^{T_A} &= \sum_{ijmn} \theta_{ijmn} |j\rangle_A \langle i| \ |m\rangle_R \langle n| \, . \end{aligned} \tag{2.4.15}$$

Due to the linearity of Φ, one could easily extend (2.4.13) to the mixed state case:

$$\Phi(\theta_A) = d \, \mathrm{tr}_R \left(\theta_R \left(\rho_\Phi\right)^{T_A} \right) \tag{2.4.16}$$

2.5 Complementary channels

The Stinespring dilation 2.4.2 allows to define another type of quantum channels; in fact, one may wonder what happens when one traces the dilation of a state over the output system instead of the environment. This leads to the definition of the *complementary channels*, which act as the "output state of the environment".

$$\tilde{\Phi} \left(\rho_A\right) \equiv \mathrm{tr}_B \left(U_{BE \leftarrow AE} \left(\rho_A |0\rangle_E \langle 0| \right) U^\dagger_{BE \leftarrow AE} \right) \in \sigma\left(\mathcal{H}_E\right) \tag{2.5.1}$$

Complementary channels, just as their "standard" counterparts, are LCPT maps. In Figure 2.5.1 the reader can find a schematic depiction of quantum channels and complementary channels.

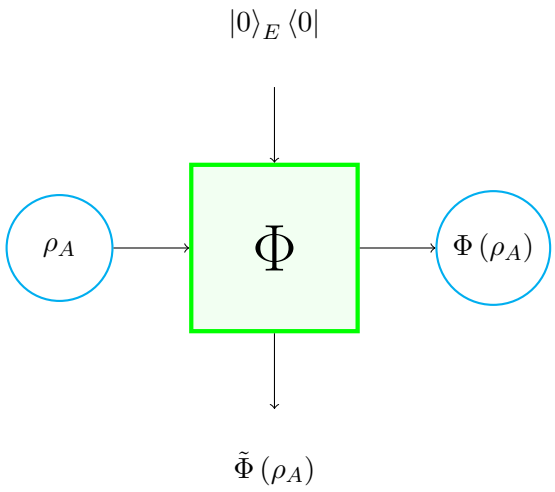

Figure 2.5.1: The quantum channel Φ depicted as a "black box" that takes as inputs ρ_S from the system S and $|0\rangle_E \langle 0|$ while it outputs $\Phi(\rho_S)$ in S and $\tilde{\Phi}(\rho_S)$ in E.

Complementary channel from Kraus representation

It is possible to find the complementary channel from a Kraus set by employing (2.4.6) into (2.5.1), yielding:

$$\tilde{\Phi}(\rho) = \sum_{ij} \operatorname{tr}\left(K_i \rho K_j^\dagger\right) |i\rangle_E \langle j| \tag{2.5.2}$$

Different Kraus representations correspond to different complementary channel, which are unitarily equivalent; in fact, given the Kraus sets $\mathcal{K}, \mathcal{K}'$:

$$\begin{aligned} \tilde{\Phi}(\rho) &= \sum_{ij} \operatorname{tr}\left(K_i \rho K_j^\dagger\right) |i\rangle_E \langle j| \\ \tilde{\Phi}'(\rho) &= \sum_{ij} \operatorname{tr}\left(K'_i \rho K'^\dagger_j\right) |e_i\rangle_E \langle e_j| \end{aligned} \tag{2.5.3}$$

Suppose $\mathcal{K}, \mathcal{K}'$, satisfy (2.4.8), then defining the isometry $U \equiv \mathcal{U}_{ij} |e_i\rangle_E \langle j|$, one could verify that:

$$\tilde{\Phi}'(\rho) = U \tilde{\Phi}(\rho) U^\dagger \tag{2.5.4}$$

2.6 Degradability and antidegradability

A quantum channel Φ is said to be *degradable* if and only if, given its complementary channel $\tilde{\Phi}$, there exists a LCPT map Λ such that the composition $\Lambda \circ \Phi$ is equal to the complementary channel $\tilde{\Phi}$:

$$\Phi \text{ is degradable} \Leftrightarrow \exists \Lambda \text{ LCPT s.t. } \tilde{\Phi} = \Lambda \circ \Phi \tag{2.6.1}$$

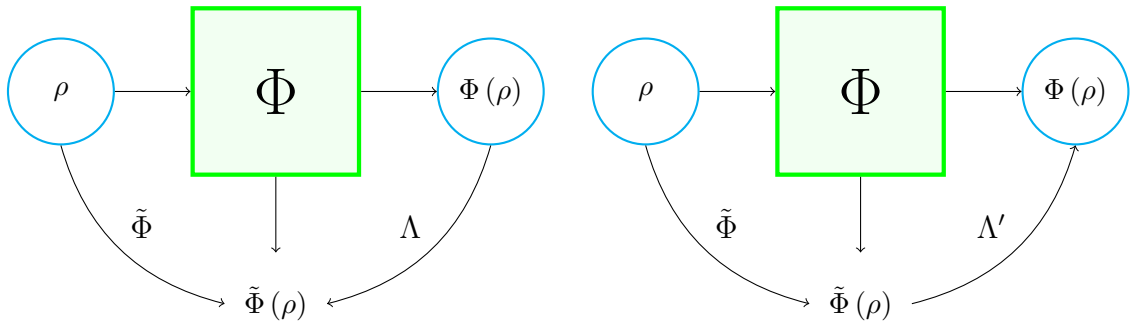

(a) Degradability of Φ **(b)** Antidegradability of Φ

Figure 2.6.1: On the left, a visual representation for the degradability condition given in (2.6.1); on the right, a visual representation for the antidegradability condition given in (2.6.2);

Conversely Φ is said to be *antidegradable* if and only if there exists a LCPT map Λ' such that the composition $\Lambda' \circ \tilde{\Phi}$ is equal to the channel Φ:

$$\Phi \text{ is antidegradable} \Leftrightarrow \exists \Lambda' \text{ LCPT s.t. } \Phi = \Lambda' \circ \tilde{\Phi}, \tag{2.6.2}$$

Figure 2.6.1 provides a visual representation of the degradability and antidegradability conditions outlined in this section.

2.7 Covariant channels

Consider a quantum channel $\Phi : \sigma(\mathcal{H}_A) \mapsto \sigma(\mathcal{H}_B)$ and a group $\mathfrak{G}$ which has unitary representations on $\mathcal{H}_A$, $\mathcal{H}_B$ and the environment $\mathcal{H}_E$, so that $\forall g \in \mathfrak{G}, \exists U_g^X$ unitary operator on $\mathcal{H}_X$. The channel Φ is called *covariant* under the action of $\mathfrak{G}$ if:

$$\Phi\left(U_g^A \rho U_g^{A\dagger}\right) = U_g^B \Phi(\rho) U_g^{B\dagger} \quad \forall g \in \mathfrak{G}, \forall \rho \in \sigma(\mathcal{H}_A) \tag{2.7.1}$$

Define $\tilde{\Phi}$ as the complementary channel of Φ; if Φ satisfies (2.7.1), then [Hol07] also its complementary channel must be covariant under the same group $\mathfrak{G}$:

$$\tilde{\Phi}\left(U_g^A \rho U_g^{A\dagger}\right) = U_g^E \tilde{\Phi}(\rho) U_g^{E\dagger} \quad \forall g \in \mathfrak{G}, \forall \rho \in \sigma(\mathcal{H}_A) \tag{2.7.2}$$

$$\Phi \text{ covariant under } \mathfrak{G} \Rightarrow \tilde{\Phi} \text{ covariant under } \mathfrak{G} \tag{2.7.3}$$

2.8 Shannon entropy

In this section, the basic tool that allows for the study of (classical) information will be introduced. Given a probability distribution $X = \{p_x\}_x$, the *Shannon entropy* (or

classical entropy) is defined as:

$$H(X) \equiv -\sum_x p_x \log_2 p_x \tag{2.8.1}$$

From the Shannon entropy, a number of information theoretic quantities can be derived, as exposed in what follows. It is important to note that, if for some x_0 one finds $p_{x_0} = 0$, one needs to set a convention to treat the indefinite form of $0 \log_2 0$ found in (2.8.1). Therefore, in the context of entropies, the reader needs to assume:

$$0 \log_2 0 \equiv 0 \tag{2.8.2}$$

One can think of the Shannon entropy as the "classical information" content that can be gained by measuring the system.

Classical relative entropy

The classical relative entropy provides a way to measure the closeness of two probability distributions $X = \{p_x\}_x$ and $Y = \{q_x\}_x$, which are defined over the same indexes. The relative entropy is defined as:

$$H(p_x||q_x) \equiv -H(X) - \sum_x p_x \log_2 q_x = \sum_x p_x \log_2 \frac{p_x}{q_x}. \tag{2.8.3}$$

An important property of the classical relative entropy is its non-negativity:

$$H(p_x||q_x) \geq 0 \tag{2.8.4}$$

Using this property, it is possible to find an upper bound for the Shannon entropy. In fact, using $q_x = 1/d \ \forall x$:

$$H(p_x||1/d) = \log_2 d - H(X) \geq 0 \Rightarrow H(X) \leq \log_2 d \tag{2.8.5}$$

This upper bound is achievable by selecting $p_x = 1/d \ \forall x$.

Joint classical entropy

Given a pair of random variables x, y and a probability distribution over those variables $XY = \{p(x,y)\}_{x,y}$, then the *joint classical entropy* is a natural extension of (2.8.1):

$$H(XY) \equiv -\sum_{x,y} p(x,y) \log_2 p(x,y) \tag{2.8.6}$$

Classical conditional entropy

In the case of two random variables x, y, the knowledge of one of those variables, for example y, changes the information content that can be gained by measuring the system; this quantity is represented by the *conditional entropy*:

$$H(X|Y) \equiv H(XY) - H(Y) \tag{2.8.7}$$

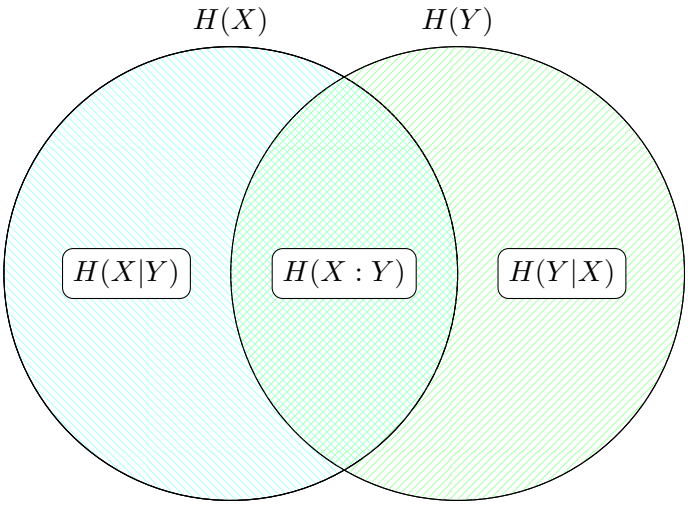

Figure 2.8.1: "Venn" diagram depicting the relationships between the various classical entropic quantities

Classical mutual information

The *mutual information* measures the information content in XY accessible to both the observers that only have access to either X or Y:

$$\begin{aligned} H(X:Y) &\equiv H(X) + H(Y) - H(XY) \\ H(X:Y) &\equiv H(X) - H(X|Y) \end{aligned} \tag{2.8.8}$$

Basic properties of entropic quantities

- The joint entropy and the mutual information are symmetric in their inputs.

$$\begin{aligned} H(XY) &= H(YX) \\ H(X:Y) &= H(Y:X) \end{aligned} \tag{2.8.9}$$

- The conditional entropy is non negative, which implies that the mutual information is not bigger than the Shannon entropy of one of its inputs

- ...

All the relationships between the quantities listed above can be (improperly) visually derived using the Venn diagram drawn in Figure 2.8.1; the diagram provides a very powerful mnemonic device that, sadly, does not work in the quantum case.

2.9 Von Neumann entropy

The quantum equivalent of the Shannon entropy in (2.8.1) is the Von Neumann entropy, defined by:

$$S(\rho) \equiv -\operatorname{tr}(\rho \log_2 \rho) \tag{2.9.1}$$

where ρ is a quantum state. The $\log_2$ in (2.9.1) is the logarithm base 2 of a matrix; formally speaking, it is the inverse operator of taking the power of that matrix base 2, while practically speaking, $\log_2 \theta$ returns a matrix θ' obtained by taking the element-wise $\log_2$ of θ in its diagonal basis and then transforming back to the original basis for θ. Since the trace operator is invariant under change of basis, this means that, denoting with $\{\lambda_x\}_x$ the eigenvalues of ρ, (2.9.1) can be reduced to the form of (2.8.1):

$$S(\rho) = -\sum_x \lambda_x \log_2 \lambda_x, \tag{2.9.2}$$

(2.8.2) still holds.

2.10 Quantum capacity

3

Previous research on finite dimensional lossy channels

As already stated in 1, the purpose of this thesis work is the computation of some capacity functionals for a specific family of quantum channels, called Multi-level Amplitude Damping (MAD) channels; the previous research on MAD channels is exposed in the present chapter.

3.1 Amplitude Damping Channels

Amplitude Damping Channels (see for example [NC10] page 380), or ADC's, are qubit-to-qubit channels defined by the Kraus set:

$$K_0 \equiv |0\rangle\langle 0| + \sqrt{1-\gamma}\,|1\rangle\langle 1| \quad K_1 \equiv \sqrt{\gamma}\,|0\rangle\langle 1|\,, \tag{3.1.1}$$

where γ is a real parameter satisfying $0 \leq \gamma \leq 1$; it completely identifies an ADC. Given an input density matrix ρ:

$$\rho = \begin{pmatrix} \rho_{00} & \rho_{01} \\ \rho_{01}^* & \rho_{11} \end{pmatrix}, \tag{3.1.2}$$

the corresponding output state of an ADC is:

$$\begin{aligned} \mathrm{ADC}_\gamma(\rho) &\equiv K_0 \rho K_0^\dagger + K_1 \rho K_1^\dagger \\ \mathrm{ADC}_\gamma(\rho) &= \begin{pmatrix} \rho_{00} + \gamma\rho_{11} & \sqrt{1-\gamma}\rho_{01} \\ \sqrt{1-\gamma}\rho_{01}^* & (1-\gamma)\rho_{11} \end{pmatrix} \end{aligned} \tag{3.1.3}$$

For a detailed review on the quantum capacity, classical and quantum entangled assisted capacity, and classical capacity of ADC's see [GF05]. In the present section, a more in-depth analysis will be given only for the quantum capacity (and, consequently, also for the classical private capacity). Upper and lower bounds for the two-way capacity of ADC's can be obtained following the results illustrated in **??**.

3.1.a Composition of ADC's

Consider a composition $\mathrm{ADC}_{\gamma''} \circ \mathrm{ADC}_{\gamma'}$, its output channel is given by:

$$\mathrm{ADC}_{\gamma''} \circ \mathrm{ADC}_{\gamma'}(\rho) = \begin{pmatrix} \rho_{00} + (\gamma' + \gamma'' - \gamma'\gamma'')\rho_{11} & \sqrt{(1-\gamma')(1-\gamma'')}\rho_{01} \\ \sqrt{(1-\gamma')(1-\gamma'')}\rho_{01}^* & (1-\gamma')(1-\gamma'')\rho_{11} \end{pmatrix} \tag{3.1.4}$$

One could define a new parameter $\gamma = \gamma' + \gamma''(1-\gamma')$, so that $\mathrm{ADC}_{\gamma''} \circ \mathrm{ADC}_{\gamma'}(\rho) = \mathrm{ADC}_{\gamma}(\rho)$. This implies that ADC's are closed under composition, and the composition rules are:

$$\begin{gathered} \mathrm{ADC}_{\gamma} = \mathrm{ADC}_{\gamma''} \circ \mathrm{ADC}_{\gamma'} \\ \gamma = \gamma' + \gamma''(1-\gamma') \geq \gamma', \gamma'' \end{gathered} \tag{3.1.5}$$

Notice that these composition rules, coupled with the bottleneck inequalities **??**, imply that any capacity functional $\mathfrak{C}$ for ADC's must be monotonous non-increasing for increasing values of γ:

$$\mathfrak{C}\left(\mathrm{ADC}_{\gamma}\right) \leq \mathfrak{C}\left(\mathrm{ADC}_{\gamma'}\right) \quad \gamma \geq \gamma' \tag{3.1.6}$$

3.1.b Complementary channel of an ADC

Equation (2.5.2) can be used to find the output of the complementary channel of an ADC given an input matrix ρ of the form (3.1.2):

$$\widetilde{\mathrm{ADC}}_{\gamma}(\rho) = \begin{pmatrix} \rho_{00} + (1-\gamma)\rho_{11} & \sqrt{\gamma}\rho_{01} \\ \sqrt{\gamma}\rho_{01}^* & \gamma\rho_{11} \end{pmatrix} \tag{3.1.7}$$

From (3.1.7) and (3.1.3), it is apparent that:

$$\mathrm{ADC}_{1-\gamma} = \widetilde{\mathrm{ADC}}_{\gamma} \tag{3.1.8}$$

3.1.c Degradability and antidegradability

The conditions (2.6.1) and (2.6.2) define what it means for a generic channel Φ to be, respectively, degradable or antidegradable. In the context of Amplitude Damping Channels, one finds, from (3.1.8), that the degradability condition reduces to:

$$\exists \Lambda : \mathrm{ADC}_{1-\gamma} = \Lambda \circ \mathrm{ADC}_{\gamma}, \tag{3.1.9}$$

while the antidegradability condition becomes:

$$\exists \Lambda' : \mathrm{ADC}_{\gamma} = \Lambda' \circ \mathrm{ADC}_{1-\gamma}. \tag{3.1.10}$$

Heuristically speaking, it would make sense if Λ and Λ' in (3.1.9) and (3.1.10) were both ADC's themselves. Following this hypothesis, one could rewrite (3.1.9) as:

$$\exists \lambda, 0 \leq \lambda \leq 1 : \mathrm{ADC}_{1-\gamma} = \mathrm{ADC}_{\lambda} \circ \mathrm{ADC}_{\gamma}, \tag{3.1.11}$$

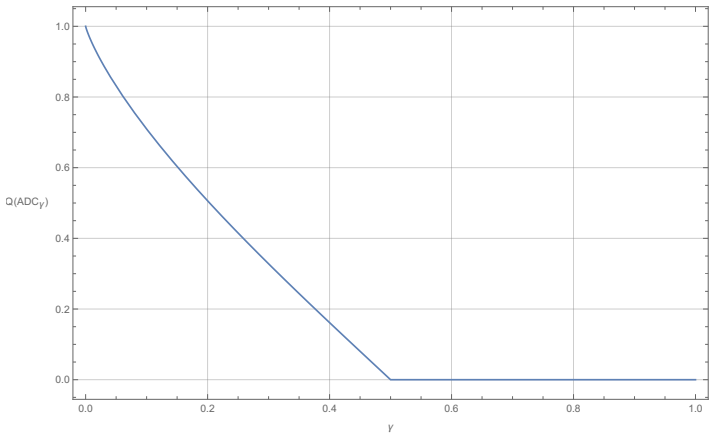

Figure 3.1.1: Quantum capacity for an Amplitude Damping Channel ADC_γ as a function of the parameter γ. Notice that (3.1.6) is satisfied.

Employing (3.1.5) into (3.1.11), one finds:

$$\lambda = \frac{1-2\gamma}{1-\gamma}. \tag{3.1.12}$$

In order for λ to satisfy $0 \leq \lambda \leq 1$, one needs to set the condition $0 \leq \gamma \leq 1/2$; therefore, if $0 \leq \gamma \leq 1/2$ the channel ADC_γ is degradable. One could also follow this line of reasoning in order to find an antidegradability condition; in fact, assuming that the antidegrading channel is itself an ADC, one could rewrite (3.1.10) as:

$$\exists \lambda', 0 \leq \lambda' \leq 1 : \mathrm{ADC}_\gamma = \mathrm{ADC}_{\lambda'} \circ \mathrm{ADC}_{1-\gamma}, \tag{3.1.13}$$

This leads to:

$$\lambda' = \frac{2\gamma - 1}{\gamma} \tag{3.1.14}$$

Therefore, ADC_γ is antidegradable if $1/2 \leq \gamma \leq 1$. This means that ADC's are either degradable or antidegradable:

$$\begin{cases} 0 \leq \gamma \leq 1/2 \Rightarrow \mathrm{ADC}_\gamma \text{ is degradable} \\ 1/2 \leq \gamma \leq 1 \Rightarrow \mathrm{ADC}_\gamma \text{ is antidegradable} \end{cases} \tag{3.1.15}$$

3.1.d Quantum Capacity of ADC's

Following the result (3.1.15), the quantum capacity of ADC's turns out to be relatively easy to compute. In fact, for $1/2 \leq \gamma \leq 1$, since the channel is antidegradable, the quantum capacity of ADC_γ is 0, while for $0 \leq \gamma \leq 1/2$, due to the property of degradable channels **??**, the quantum capacity of ADC_γ corresponds to the maximum of the coherent information over all possible inputs:

$$Q\left(\mathrm{ADC}_\gamma\right) = Q^{(1)}\left(\mathrm{ADC}_\gamma\right) = \max_{\rho \in \sigma(\mathcal{H}_2)} I_c\left(\rho, \mathrm{ADC}_\gamma\right) \quad \forall 0 \leq \gamma \leq 1/2 \tag{3.1.16}$$

Thanks to a property that MAD channels present for every dimension d (see **??**), the maximum in (3.1.16) can be computed over all diagonal density matrices $\rho^{(diag)}$:

$$\rho^{(diag)} \equiv p\,|0\rangle\langle 0| + (1-p)\,|1\rangle\langle 1| \tag{3.1.17}$$

$$\begin{aligned}\max_{\rho^{(diag)}\in\sigma(\mathcal{H}_2)} I_c\left(\rho, \mathrm{ADC}_\gamma\right) = \max_p\{ &-(1-p)(1-\gamma)\log_2((1-p)(1-\gamma)) \\ &-(\gamma+p(1-\gamma))\log_2(\gamma+p(1-\gamma)) \\ &+(1-\gamma(1-p))\log_2(1-\gamma(1-p)) \\ &+\gamma(1-p)\log_2(\gamma(1-p))\}\end{aligned} \tag{3.1.18}$$

TODO aggiusta. The right-hand side of (3.1.18) can be computed using a numerical evaluation (see **??** for details), obtaining the plot reported in Figure 3.1.1.

3.2 Partially Coherent Direct Sum channels

In [CG21b], the authors analyze channels of the form:

$$\Phi_{\mathrm{CC}}(\Theta_{\mathrm{CC}}) \equiv \left[\begin{array}{c|c} \Phi_{\mathrm{AA}}\left(\Theta_{\mathrm{AA}}\right) & \Phi_{\mathrm{AB}}^{(\mathrm{off})}\left(\Theta_{\mathrm{AB}}\right) \\ \hline \Phi_{\mathrm{BA}}^{(\mathrm{off})}\left(\Theta_{\mathrm{BA}}\right) & \Phi_{\mathrm{BB}}\left(\Theta_{\mathrm{BB}}\right) \end{array}\right] \tag{3.2.1}$$

$$\Theta_{\mathrm{CC}} \equiv \left[\begin{array}{c|c} \Theta_{\mathrm{AA}} & \Theta_{\mathrm{AB}} \\ \hline \Theta_{\mathrm{BA}} & \Theta_{\mathrm{BB}} \end{array}\right];$$

these are called Partially Coherent Direct Sum (PCDS) channels. For this type of channels, it was shown that:

$$\Phi_{\mathrm{CC}} \text{ is degradable} \Leftrightarrow \Phi_{\mathrm{AA}}, \Phi_{\mathrm{BB}} \text{ are both degradable} \tag{3.2.2}$$

If Φ_{CC} is degradable, its quantum capacity presents an upper bound:

$$Q\left(\Phi_{\mathrm{CC}}\right) \leq \log_2\left(2^{Q(\Phi_{\mathrm{AA}})} + 2^{Q(\Phi_{\mathrm{BB}})}\right) \tag{3.2.3}$$

Special case of $\Phi_{\mathrm{BB}} = \mathbb{1}_{\mathrm{BB}}$

Suppose Φ_{BB} is the identity channel on $\mathcal{H}_{\mathrm{B}}$, $\mathbb{1}_{\mathrm{BB}}$; the upper bound (3.2.3) becomes:

$$Q\left(\Phi_{\mathrm{CC}}\right) \leq \log_2\left(2^{Q(\Phi_{\mathrm{AA}})} + d_{\mathrm{B}}\right) \tag{3.2.4}$$

where $d_{\mathrm{B}} = \dim \mathcal{H}_{\mathrm{B}}$. In this case, a lower bound for $Q\left(\Phi_{\mathrm{CC}}\right)$ can also be found:

$$Q\left(\Phi_{\mathrm{CC}}\right) \geq \log_2\left(1 + d_{\mathrm{B}}\right) \tag{3.2.5}$$

If the degradable channel Φ_{AA} has null quantum capacity, then the upper bound (3.2.4) and the lower bound (3.2.5) coincide:

$$Q\left(\Phi_{\mathrm{AA}}\right) = 0 \Rightarrow Q\left(\Phi_{\mathrm{CC}}\right) = \log_2\left(1 + d_{\mathrm{B}}\right) \tag{3.2.6}$$

3.3 3-dimensional Multi-level Amplitude Damping channels

Multi-level Amplitude Damping channels are the generalization to the qudit case of ADC channels; they were first explored in the article [CG21a], which is summarized in the present section.

3.3.a Settings for d-dimensional MAD channels

The paper [CG21a] outlines the settings for a d-dimensional MAD channel, which are also reported here for the sake of completeness. Given a d-dimensional Hilbert space $\mathcal{H}$, spanned by the basis $\{|i\rangle\}_i$, for $i = 0, ..., d-1$, the MAD channel has a minimal Kraus representation given by the Kraus operators:

$$\begin{aligned} K_{ij} &\equiv \sqrt{\gamma_{ji}}\,|i\rangle\langle j| \quad 0 \leq i < j \leq d-1 \\ K_{00} &\equiv \sum_{j=0}^{d-1} \sqrt{\gamma_{jj}}\,|j\rangle\langle j|\,. \end{aligned} \tag{3.3.1}$$

The γ_{ji}'s in (3.3.1) describe the probabilities of decay from level $|j\rangle$ onto level $|i\rangle$, while γ_{jj}'s describe the probabilities that level $|j\rangle$ will not decay during the transformation; as such, these are real quantities satisfying:

$$\gamma_{jj} \equiv 1 - \sum_{i=0}^{j-1} \gamma_{ji} \tag{3.3.2}$$

$$\begin{cases} 0 \leq \gamma_{ji} \leq 1 \quad \forall\, 0 \leq i < j \leq d-1 \\ 0 \leq \gamma_{jj} \leq 1 \quad \forall\, 0 \leq j \leq d-1 \\ \gamma_{ji} = 0 \quad \forall i > j \end{cases} \tag{3.3.3}$$

These quantities,which will be called *transition probabilities* in what follows, can be grouped into a matrix, which will be called *transition matrix*, defined by:

$$\Gamma \equiv \mathbb{1}_d + \sum_{j=1}^{d-1}\sum_{i=0}^{j-1} \gamma_{ji}\,|j\rangle\langle i| - \sum_{j=1}^{d-1}\sum_{i=0}^{j-1} \gamma_{ji}\,|j\rangle\langle j| \tag{3.3.4}$$

where $\mathbb{1}_d$ is the d-dimensional identity operator. There is a one-to-one relation between a specific MAD channel and its transition matrix, so that, given a transition matrix Γ, it is possible to identify the corresponding MAD channel by Φ_Γ:

$$\Phi_\Gamma \sim \Gamma \tag{3.3.5}$$

Finally, given an input $\rho \in \sigma(\mathcal{H})$, a MAD channel Φ_Γ outputs the state:

$$\Phi_\Gamma(\rho) = K_{00}\rho K_{00}^\dagger + \sum_{j=1}^{d-1}\sum_{i=0}^{j-1} K_{ij}\rho K_{ij}^\dagger. \tag{3.3.6}$$

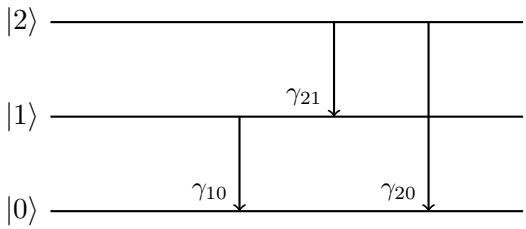

Figure 3.3.1: MAD channels represent decay processes, where each level of a system has a fixed probability of decaying onto a lower level. Here, a schematic depiction of a 3-dimensional MAD is reported

Which, in terms of transition probabilities, translates to:

$$\Phi_\Gamma(\rho) = \sum_{m=0}^{d-1}\sum_{n=0}^{d-1}\sqrt{\gamma_{mm}\gamma_{nn}}\rho_{mn}\,|m\rangle\langle n| + \sum_{j=1}^{d-1}\sum_{i=0}^{j-1}\gamma_{ji}\rho_{ii}\,|i\rangle\langle i| \tag{3.3.7}$$

3.3.b Settings for 3-dimensional MAD channels

Set $d = 3$; a generic 3-dimensional MAD channel $\Phi_\Gamma^{(3)}$ is uniquely identified by its transition matrix Γ:

$$\Gamma = \begin{pmatrix} 1 & 0 & 0 \\ \gamma_{10} & 1-\gamma_{10} & 0 \\ \gamma_{20} & \gamma_{21} & 1-\gamma_{20}-\gamma_{21} \end{pmatrix}, \tag{3.3.8}$$

while the Kraus set for $\Phi_\Gamma^{(3)}$, taken from (3.3.1), is:

$$K_{00} = \begin{pmatrix} 1 & 0 & 0 \\ 0 & \sqrt{1-\gamma_{10}} & 0 \\ 0 & 0 & \sqrt{1-\gamma_{20}-\gamma_{21}} \end{pmatrix}$$
$$K_{01} = \begin{pmatrix} 0 & \sqrt{\gamma_{10}} & 0 \\ 0 & 0 & 0 \\ 0 & 0 & 0 \end{pmatrix} \quad K_{02} = \begin{pmatrix} 0 & 0 & \sqrt{\gamma_{20}} \\ 0 & 0 & 0 \\ 0 & 0 & 0 \end{pmatrix} \quad K_{12} = \begin{pmatrix} 0 & 0 & 0 \\ 0 & 0 & \sqrt{\gamma_{21}} \\ 0 & 0 & 0 \end{pmatrix} \tag{3.3.9}$$

The transition probabilities $\gamma_{10}, \gamma_{20}, \gamma_{21}$ satisfy the conditions:

$$\begin{cases} 0 \le \gamma_{10}, \gamma_{20}, \gamma_{21} \le 1 \\ 0 \le \gamma_{20} + \gamma_{21} \le 1 \end{cases} \tag{3.3.10}$$

Given an input density matrix ρ:

$$\rho = \begin{pmatrix} \rho_{00} & \rho_{01} & \rho_{02} \\ \rho_{01}^* & \rho_{11} & \rho_{12} \\ \rho_{02}^* & \rho_{12}^* & \rho_{22} \end{pmatrix}, \tag{3.3.11}$$

the output state of $\Phi_\Gamma^{(3)}$ is:

$$\Phi_\Gamma^{(3)}(\rho) = \begin{pmatrix} \gamma_{10}\rho_{11} + \gamma_{20}\rho_{22} + \rho_{00} & \sqrt{1-\gamma_{10}}\rho_{01} & \sqrt{1-\gamma_{20}-\gamma_{21}}\rho_{02} \\ \sqrt{1-\gamma_{10}}\rho_{01}^* & (1-\gamma_{10})\,\rho_{11} + \gamma_{21}\rho_{22} & \sqrt{1-\gamma_{10}}\sqrt{1-\gamma_{20}-\gamma_{21}}\rho_{12} \\ \sqrt{1-\gamma_{20}-\gamma_{21}}\rho_{02}^* & \sqrt{1-\gamma_{10}}\sqrt{1-\gamma_{20}-\gamma_{21}}\rho_{12}^* & (1-\gamma_{20}-\gamma_{21})\,\rho_{22} \end{pmatrix}, \quad (3.3.12)$$

while the output state of the complementary channel $\tilde{\Phi}_\Gamma^{(3)}$ is

$$\tilde{\Phi}_\Gamma^{(3)}(\rho) = \begin{pmatrix} (1-\gamma_{10})\,\rho_{11} + (1-\gamma_{20}-\gamma_{21})\,\rho_{22} + \rho_{00} & \sqrt{\gamma_{10}}\rho_{01} & \sqrt{\gamma_{20}}\rho_{02} & \sqrt{1-\gamma_{10}}\sqrt{\gamma_{21}}\rho_{12} \\ \sqrt{\gamma_{10}}\rho_{01}^* & \gamma_{10}\rho_{11} & \sqrt{\gamma_{10}}\sqrt{\gamma_{20}}\rho_{12} & 0 \\ \sqrt{\gamma_{20}}\rho_{02}^* & \sqrt{\gamma_{10}}\sqrt{\gamma_{20}}\rho_{12}^* & \gamma_{20}\rho_{22} & 0 \\ \sqrt{1-\gamma_{10}}\sqrt{\gamma_{21}}\rho_{12}^* & 0 & 0 & \gamma_{21}\rho_{22} \end{pmatrix}. \quad (3.3.13)$$

Refer to Figure 3.3.1 for a schematic representation of 3-dimensional MAD channels.

3.3.c Composition rules

The paper [CG21a] shows that MAD channels in $d = 3$ are closed under channel composition, which means that the composition of two 3-dimensional MAD channels is itself a 3-dimensional MAD channel. This result can be generalized to an arbitrary dimension d, as shown in Section 4.2. The composition rules of 3-dimensional MAD channels are:

$$\Phi_\Gamma^{(3)} = \Phi_{\Gamma''}^{(3)} \circ \Phi_{\Gamma'}^{(3)}$$
$$\begin{cases} \gamma_{10} = \gamma'_{10} + \gamma''_{10}\,(1-\gamma'_{10}) \\ \gamma_{20} = \gamma'_{20} + \gamma''_{20}\,(1-\gamma'_{20}) + \gamma'_{21}\gamma''_{10} \\ \gamma_{21} = \gamma'_{21}\,(1-\gamma''_{10}) + \gamma''_{21}\,(1-\gamma'_{20}-\gamma'_{21}) \end{cases} \quad (3.3.14)$$

where $\gamma_{ji} = \langle j|\Gamma|i\rangle\,, \gamma'_{ji} = \langle j|\Gamma'|i\rangle\,, \gamma''_{ji} = \langle j|\Gamma''|i\rangle$. Intuitively, the composition rules (3.3.14) suggest that the transition probability γ_{ji}, resulting from a composition of two MAD channels, is the sum of the probabilities all the possible two-step decay "paths" from $|j\rangle$ to $|i\rangle$. This idea is corroborated in Section 4.2.

3.3.d Covariance

Consider a d-dimensional MAD channel $\Phi_\Gamma : \sigma(\mathcal{H}) \mapsto \sigma(\mathcal{H})$ and consider the d-dimensional unitary matrices U diagonal in the computational basis:

$$U \equiv \sum_{j=0}^{d-1} e^{i\varphi_j}\,|j\rangle\langle j| \quad \varphi_j \in \mathbb{R} \quad \forall j. \quad (3.3.15)$$

It is possible to verify that Φ_Γ is covariant under the action of the group of unitary operators whose elements in the representation in $\mathcal{H}$ are in the form (3.3.15), i.e.:

$$\Phi_\Gamma(U\rho U^\dagger) = U\Phi_\Gamma(\rho)U^\dagger. \quad (3.3.16)$$

3.3.e Maximum of coherent information for degradable MAD channels

If a channel Φ is covariant under the action of a group $\mathfrak{G}$, by employing (2.7.3) and the invariance of the von Neumann entropy under unitary operations, one obtains:

$$\begin{aligned} &\Phi : \sigma(\mathcal{H}_A) \mapsto \sigma(\mathcal{H}_B) \text{ covariant under } \mathfrak{G} \\ &\Rightarrow I_c\left(U_g^A \rho U_g^{A\dagger}, \Phi\right) = I_c(\rho, \Phi) \end{aligned} \tag{3.3.17}$$

Furthermore, consider the state $\bar{\rho}_{\mathfrak{G}}$ obtained by taking the average over all the applications of elements $g \in \mathfrak{G}$ upon the input state ρ:

$$\bar{\rho}_{\mathfrak{G}} \equiv \int \mathrm{d}\mu_g U_g^A \rho U_g^{A\dagger}, \tag{3.3.18}$$

where μ_g is a probability distribution over the group $\mathfrak{G}$; if Φ is degradable, by the property **??** the coherent information is concave in the input state ρ, therefore:

$$I_c(\bar{\rho}_{\mathfrak{G}}, \Phi) \geq \int \mathrm{d}\mu_g I_c\left(U_g^A \rho U_g^{A\dagger}, \Phi\right) \overset{(3.3.17)}{=} I_c(\rho, \Phi) \tag{3.3.19}$$

Regarding MAD channels Φ_Γ, as seen in (3.3.16), $\mathfrak{G}$ could be replaced by the group of unitary operators diagonal in the computational basis; in this case, $\bar{\rho}_{\mathfrak{G}}$ corresponds to a diagonal density matrices $\rho^{(diag)}$, so that (3.3.19) becomes:

$$I_c\left(\rho^{(diag)}, \Phi_\Gamma\right) \geq I_c(\rho, \Phi_\Gamma) \tag{3.3.20}$$

Hence, for degradable MAD channels, the search for the maximum over input states in (**??**) can be restricted to diagonal input states:

$$Q(\Phi_\Gamma) = Q^{(1)}(\Phi_\Gamma) \equiv \max_\rho I_c(\rho, \Phi_\Gamma) \overset{(3.3.20)}{=} \max_{\rho^{(diag)}} I_c\left(\rho^{(diag)}, \Phi_\Gamma\right) \tag{3.3.21}$$

3.3.f Single decays

Consider the single decay channels $\Phi^{(3)}_{\Gamma_{10}(\gamma)}, \Phi^{(3)}_{\Gamma_{20}(\gamma)}, \Phi^{(3)}_{\Gamma_{21}(\gamma)}$, whose transition matrices present the same single transition probability:

$$\Gamma_{10}(\gamma) \equiv \begin{pmatrix} 1 & 0 & 0 \\ \gamma & 1-\gamma & 0 \\ 0 & 0 & 1 \end{pmatrix} \Gamma_{20}(\gamma) \equiv \begin{pmatrix} 1 & 0 & 0 \\ 0 & 1 & 0 \\ \gamma & 0 & 1-\gamma \end{pmatrix} \Gamma_{21}(\gamma) \equiv \begin{pmatrix} 1 & 0 & 0 \\ 0 & 1 & 0 \\ 0 & \gamma & 1-\gamma \end{pmatrix} \tag{3.3.22}$$

Define the swap matrices:

$$U_{10} \equiv \begin{pmatrix} 0 & 1 & 0 \\ 1 & 0 & 0 \\ 0 & 0 & 1 \end{pmatrix}, \quad U_{21} \equiv \begin{pmatrix} 1 & 0 & 0 \\ 0 & 0 & 1 \\ 0 & 1 & 0 \end{pmatrix}; \tag{3.3.23}$$

the channels $\Phi^{(3)}_{\Gamma_{10}(\gamma)}, \Phi^{(3)}_{\Gamma_{20}(\gamma)}, \Phi^{(3)}_{\Gamma_{21}(\gamma)}$ can be mapped into each other via unitary channels corresponding to (3.3.23):

$$\mathcal{U}_{10}(\bullet) \equiv U_{10} \bullet U_{10} \quad \mathcal{U}_{21}(\bullet) \equiv U_{21} \bullet U_{21} \tag{3.3.24}$$

$$\begin{aligned} \mathcal{U}_{21} \circ \Phi^{(3)}_{\Gamma_{10}(\gamma)} \circ \mathcal{U}_{21} &= \Phi^{(3)}_{\Gamma_{20}(\gamma)} \\ \mathcal{U}_{10} \circ \Phi^{(3)}_{\Gamma_{20}(\gamma)} \circ \mathcal{U}_{10} &= \Phi^{(3)}_{\Gamma_{21}(\gamma)} \\ \mathcal{U}_{10} \circ \mathcal{U}_{21} \circ \Phi^{(3)}_{\Gamma_{10}(\gamma)} \circ \mathcal{U}_{21} \circ \mathcal{U}_{10} &= \Phi^{(3)}_{\Gamma_{21}(\gamma)} \end{aligned} \tag{3.3.25}$$

From the bottleneck inequality (**??**), (3.3.25) and the invertibility of unitary channels, one can infer that $\Phi^{(3)}_{\Gamma_{10}(\gamma)}, \Phi^{(3)}_{\Gamma_{20}(\gamma)}, \Phi^{(3)}_{\Gamma_{21}(\gamma)}$ have the same capacity functionals, which means that the capacity of a single decay 3-dimensional MAD channel only depends on the transition probability, not on the specific levels involved in the decay.

The composition rules for $\Phi^{(3)}_{\Gamma_{10}(\gamma)}, \Phi^{(3)}_{\Gamma_{20}(\gamma)}, \Phi^{(3)}_{\Gamma_{21}(\gamma)}$ are very similar to those found for ADC's (3.1.5):

$$\begin{aligned} \Phi^{(3)}_{\Gamma_{ji}(\gamma)} &= \Phi^{(3)}_{\Gamma_{ji}(\gamma'')} \circ \Phi^{(3)}_{\Gamma_{ji}(\gamma')} \\ \gamma &= \gamma' + \gamma''(1-\gamma') \geq \gamma', \gamma'', \end{aligned} \tag{3.3.26}$$

where $0 \leq i < j \leq 1$.

3.3.g Monotonicity

Exploiting the composition rules derived in Subsection 3.3.c, one can infer monotonicity properties for the capacity functionals of 3-dimensional MAD channels. In fact, the relation (**??**), in the context of (3.3.14), becomes:

$$\mathfrak{C}\left(\Phi^{(3)}_{\Gamma}\right) \leq \min\left\{\mathfrak{C}\left(\Phi^{(3)}_{\Gamma'}\right), \mathfrak{C}\left(\Phi^{(3)}_{\Gamma''}\right)\right\} \tag{3.3.27}$$

Define a generic 3-dimensional MAD channel:

$$\Phi^{(3)}_{\Gamma} \equiv \Phi^{(3)}_{\Gamma(\gamma_{10},\gamma_{20},\gamma_{21})} \tag{3.3.28}$$

where the dependency of Γ in (3.3.8) on the real parameters $\gamma_{10}, \gamma_{20}, \gamma_{21}$ has been made explicit; using (3.3.14), one can find decompositions of $\Phi^{(3)}_{\Gamma(\gamma_{10},\gamma_{20},\gamma_{21})}$, whose composing channels have higher capacity than $\Phi^{(3)}_{\Gamma(\gamma_{10},\gamma_{20},\gamma_{21})}$. Some of these decompositions are reported below:

$$\Phi^{(3)}_{\Gamma(\gamma_{10},\gamma_{20},\gamma_{21})} = \Phi^{(3)}_{\Gamma(0,\gamma_{20},\gamma_{21})} \circ \Phi^{(3)}_{\Gamma(\gamma_{10},0,0)}, \tag{3.3.29}$$

$$\Phi^{(3)}_{\Gamma(\gamma_{10},\gamma_{20},\gamma_{21})} = \Phi^{(3)}_{\Gamma(0,\bar{\gamma}_{20},0)} \circ \Phi^{(3)}_{\Gamma(\gamma_{10},0,\gamma_{21})} \quad \bar{\gamma}_{20} \equiv \frac{\gamma_{20}}{1-\gamma_{21}}, \tag{3.3.30}$$

$$\Phi^{(3)}_{\Gamma(\gamma_{10},\gamma_{20},\gamma_{21})} = \Phi^{(3)}_{\Gamma(0,0,\bar{\gamma}_{21})} \circ \Phi^{(3)}_{\Gamma(\gamma_{10},\gamma_{20},0)} \quad \bar{\gamma}_{21} \equiv \frac{\gamma_{21}}{1-\gamma_{20}}, \tag{3.3.31}$$

Employing (3.3.26) into (3.3.29), (3.3.30) and (3.3.31), each single decay channel found in these decompositions is split into two new single decay channels with transition probabilities $\gamma'_{ji}, \gamma''_{ji} \leq \gamma_{ji}$:

$$\Phi^{(3)}_{\Gamma(\gamma_{10},0,0)} = \Phi^{(3)}_{\Gamma(\gamma'_1 0,0,0)} \circ \Phi^{(3)}_{\Gamma(\gamma''_{10},0,0)}, \tag{3.3.32}$$

$$\Phi^{(3)}_{\Gamma(0,\bar{\gamma}_{20},0)} = \Phi^{(3)}_{\Gamma(0,\bar{\gamma}''_{20},0)} \circ \Phi^{(3)}_{\Gamma(0,\bar{\gamma}'_{20},0)}, \tag{3.3.33}$$

$$\Phi^{(3)}_{\Gamma(0,0,\bar{\gamma}_{21})} = \Phi^{(3)}_{\Gamma(0,0,\bar{\gamma}''_{21})} \circ \Phi^{(3)}_{\Gamma(0,0,\bar{\gamma}'_{21})}. \tag{3.3.34}$$

where:

$$\bar{\gamma}''_{21} \equiv \frac{\gamma''_{21}}{1-\gamma_{20}} \quad \bar{\gamma}'_{21} \equiv \frac{\gamma'_{21}}{1-\gamma_{20}} \tag{3.3.35}$$

$$\bar{\gamma}''_{20} \equiv \frac{\gamma''_{20}}{1-\gamma_{21}} \quad \bar{\gamma}'_{20} \equiv \frac{\gamma'_{20}}{1-\gamma_{21}}. \tag{3.3.36}$$

Therefore, (3.3.29), (3.3.30) and (3.3.31) become:

$$\Phi^{(3)}_{\Gamma(\gamma_{10},\gamma_{20},\gamma_{21})} = \Phi^{(3)}_{\Gamma(\gamma'_{10},\gamma_{20},\gamma_{21})} \circ \Phi^{(3)}_{\Gamma(\gamma''_{10},0,0)} \quad \gamma'_{10} \leq \gamma_{10}, \tag{3.3.37}$$

$$\Phi^{(3)}_{\Gamma(\gamma_{10},\gamma_{20},\gamma_{21})} = \Phi^{(3)}_{\Gamma(0,\bar{\gamma}''_{20},0)} \circ \Phi^{(3)}_{\Gamma(\gamma_{10},\gamma'_{20},\gamma_{21})} \quad \gamma'_{20} \leq \gamma_{20}, \tag{3.3.38}$$

$$\Phi^{(3)}_{\Gamma(\gamma_{10},\gamma_{20},\gamma_{21})} = \Phi^{(3)}_{\Gamma(0,0,\bar{\gamma}''_{21})} \circ \Phi^{(3)}_{\Gamma(\gamma_{10},\gamma_{20},\gamma'_{21})} \quad \gamma'_{21} \leq \gamma_{21}. \tag{3.3.39}$$

Combining (3.3.37), (3.3.38) and (3.3.39) with (3.3.27), the monotonicity rules w.r.t. the transition probabilities for the capacities of 3-dimensional MAD channels are found.

$$\begin{aligned}
&\mathfrak{C}\left(\Phi^{(3)}_{\Gamma(\gamma_{10},\gamma_{20},\gamma_{21})}\right) \leq \mathfrak{C}\left(\Phi^{(3)}_{\Gamma(\gamma'_{10},\gamma_{20},\gamma_{21})}\right) \quad \forall \gamma_{10} \geq \gamma'_{10}, \\
&\mathfrak{C}\left(\Phi^{(3)}_{\Gamma(\gamma_{10},\gamma_{20},\gamma_{21})}\right) \leq \mathfrak{C}\left(\Phi^{(3)}_{\Gamma(\gamma_{10},\gamma'_{20},\gamma_{21})}\right) \quad \forall \gamma_{20} \geq \gamma'_{20}, \\
&\mathfrak{C}\left(\Phi^{(3)}_{\Gamma(\gamma_{10},\gamma_{20},\gamma_{21})}\right) \leq \mathfrak{C}\left(\Phi^{(3)}_{\Gamma(\gamma_{10},\gamma_{20},\gamma'_{21})}\right) \quad \forall \gamma_{21} \geq \gamma'_{21}.
\end{aligned} \tag{3.3.40}$$

This means that, when any transition probability of a 3-dimensional MAD channel increases, its capacity functionals decrease.

3.3.h Quantum capacity and private classical capacity

In Section 2.10 the quantum capacity of quantum channels was introduced; in most cases, it is not possible to compute the exact value of this quantity for a given channel, however, one notable exception to this rule stems from degradable channels, whose quantum capacity corresponds to the maximum over all input states of the coherent information of the channel, as seen in (**??**). Another important simplification for degradable MAD channels is provided by (**??**), which restricts the search for the maximum of the coherent

information over diagonal input states. For degradable 3-dimensional MAD channels, this translates to:

$$Q\left(\Phi_\Gamma^{(3)}\right) \overset{(??)}{=} C_p\left(\Phi_\Gamma^{(3)}\right) = \max_\rho I_c\left(\rho, \Phi_\Gamma^{(3)}\right) = \max_{p_0,p_1} I_c\left(\rho^{(diag)}, \Phi_\Gamma^{(3)}\right)$$
$$\rho^{(diag)} \equiv \begin{pmatrix} p_0 & 0 & 0 \\ 0 & p_1 & 0 \\ 0 & 0 & 1-p_0-p_1 \end{pmatrix} \quad \begin{cases} 0 \leq p_0, p_1 \leq 1 \\ 0 \leq 1-p_0-p_1 \leq 1 \end{cases} \tag{3.3.41}$$

Equation (3.3.21) (and, particularly for $d = 3$, (3.3.41)) allows for the development of a *modus operandi* for the analysis of the quantum capacity of d-dimensional MAD channels Φ_Γ:

- Find degradability and antidegradability regions for Φ_Γ.
- Compute the quantum capacity in the degradability regions using (3.3.21).
- Try to extend the computation to non-degradable zones.

The last step in this process, in the context of 3-dimensional MAD channels, will be expanded individually in each degradable zone, while a more general approach for d-dimensional MAD channels is provided in **??**.

3.3.i Degradability regions

A generic algorithm for determining the degradability regions of a d-dimensional MAD channel is offered in 4.6; it consists on finding the right-inverse map for a d-dimensional MAD channel Φ_Γ, denoted by $\Phi_\Gamma^{(-1)}$ and defined in (4.5.7), and checking the positivity of the Choi matrix C_Λ corresponding to the map:

$$\Lambda \equiv \tilde{\Phi}_\Gamma \circ \Phi_\Gamma^{-1}. \tag{3.3.42}$$

By **??**, $C_\Lambda \geq 0$ if and only if Λ is completely positive; since Λ is linear and trace preserving by construction[1], its complete positiveness would imply that it is a quantum channel, acting as the degrading channel of Φ_Γ, which, in light of this, would be a degradable channel. To simplify this computation-heavy task, a more heuristic approach is needed and provided here for the specific case of $d = 3$. Given a 3-dimensional MAD channel $\Phi_\Gamma^{(3)}$, in order to find a connecting channel $\Lambda^{(3)}$ such that:

$$\Lambda^{(3)} \circ \Phi_\Gamma^{(3)} = \tilde{\Phi}_\Gamma^{(3)} \tag{3.3.43}$$

assume that the rank of the output density matrix is greater or equal than the rank of the density matrix of the environment:

$$\text{rank}\left(\Phi_\Gamma^{(3)}(\rho)\right) \geq \text{rank}\left(\tilde{\Phi}_\Gamma^{(3)}(\rho)\right) \quad \forall\rho \tag{3.3.44}$$

[1] This is a consequence of the linearity and trace preservation of both $\Phi_\Gamma^{(-1)}$ (see (4.5.7)) and $\tilde{\Phi}_\Gamma$.

For a generic ρ, rank $\left(\Phi_{\Gamma}^{(3)}(\rho)\right) = 3$; given a minimal Kraus set $\mathcal{K}$ of a channel Φ, from (2.5.2) it can be deduced that the rank of $\tilde{\Phi}(\rho)$ corresponds to the cardinality of $\mathcal{K}$, hence, rank $\left(\tilde{\Phi}_{\Gamma}^{(3)}(\rho)\right) = 4$; the rank of the environment can be reduced to be ≤ 3 by "turning off" at least one decay, i.e. by setting at least one $\gamma_{ji} = 0$ for some $i \leq j$. This breaks down the problem to three scenarios:

1. $\gamma_{10} = 0$, in which case $\Phi_{\Gamma}^{(3)}$ is degradable for $\gamma_{20} + \gamma_{21} \leq 1/2$, see below.
2. $\gamma_{20} = 0$, in which case $\Phi_{\Gamma}^{(3)}$ is never degradable, see below.
3. $\gamma_{21} = 0$, in which case $\Phi_{\Gamma}^{(3)}$ is degradable for $\gamma_{10} \leq 1/2 \wedge \gamma_{20} \leq 1/2$, see below.

Degradability for $\gamma_{10} = 0$

The output state of $\Phi_{\Gamma(0,\gamma_{20},\gamma_{21})}^{(3)}$ is:

$$\Phi_{\Gamma(0,\gamma_{20},\gamma_{21})}^{(3)}(\rho) = \begin{pmatrix} \gamma_{20}\rho_{22} + \rho_{00} & \rho_{01} & \sqrt{1-\gamma_{20}-\gamma_{21}}\rho_{02} \\ \rho_{01}^{*} & \gamma_{21}\rho_{22} + \rho_{11} & \sqrt{1-\gamma_{20}-\gamma_{21}}\rho_{12} \\ \sqrt{1-\gamma_{20}-\gamma_{21}}\rho_{02}^{*} & \sqrt{1-\gamma_{20}-\gamma_{21}}\rho_{12}{}^{*} & (1-\gamma_{20}-\gamma_{21})\,\rho_{22} \end{pmatrix} \tag{3.3.45}$$

While the state of the environment is:

$$\tilde{\Phi}_{\Gamma(0,\gamma_{20},\gamma_{21})}^{(3)}(\rho) = \begin{pmatrix} (1-\gamma_{20}-\gamma_{21})\,\rho_{22} + \rho_{00} + \rho_{11} & \sqrt{\gamma_{20}}\rho_{02} & \sqrt{\gamma_{21}}\rho_{12} \\ \sqrt{\gamma_{20}}\rho_{02}^{*} & \gamma_{20}\rho_{22} & 0 \\ \sqrt{\gamma_{21}}\rho_{12}{}^{*} & 0 & \gamma_{21}\rho_{22} \end{pmatrix} \tag{3.3.46}$$

Given the degrading map

$$\Lambda_{\Gamma(0,\gamma_{20},\gamma_{21})}^{(3)} \equiv \tilde{\Phi}_{\Gamma(0,\gamma_{20},\gamma_{21})}^{(3)} \circ {\Phi^{(3)}}_{\Gamma(0,\gamma_{20},\gamma_{21})}^{-1}, \tag{3.3.47}$$

checking the positivity of the associated Choi matrix yields the degradability condition:

$$\gamma_{20} + \gamma_{21} \leq \frac{1}{2} \tag{3.3.48}$$

Degradability for $\gamma_{20} = 0$

The output state of $\Phi_{\Gamma(\gamma_{10},0,\gamma_{21})}^{(3)}$ is:

$$\Phi_{\Gamma(\gamma_{10},0,\gamma_{21})}^{(3)}(\rho) = \begin{pmatrix} \gamma_{10}\rho_{11} + \rho_{00} & \sqrt{1-\gamma_{10}}\rho_{01} & \sqrt{1-\gamma_{21}}\rho_{02} \\ \sqrt{1-\gamma_{10}}\rho_{01}^{*} & (1-\gamma_{10})\,\rho_{11} + \gamma_{21}\rho_{22} & \sqrt{1-\gamma_{10}}\sqrt{1-\gamma_{21}}\rho_{12} \\ \sqrt{1-\gamma_{21}}\rho_{02}^{*} & \sqrt{1-\gamma_{10}}\sqrt{1-\gamma_{21}}\rho_{12}^{*} & (1-\gamma_{21})\,\rho_{22} \end{pmatrix} \tag{3.3.49}$$

While the state of the environment is:

$$\tilde{\Phi}_{\Gamma(\gamma_{10},0,\gamma_{21})}^{(3)}(\rho) = \begin{pmatrix} (1-\gamma_{10})\,\rho_{11} + (1-\gamma_{21})\,\rho_{22} + \rho_{00} & \sqrt{\gamma_{10}}\rho_{01} & \sqrt{1-\gamma_{10}}\sqrt{\gamma_{21}}\rho_{12} \\ \sqrt{\gamma_{10}}\rho_{01}^{*} & \gamma_{10}\rho_{11} & 0 \\ \sqrt{1-\gamma_{10}}\sqrt{\gamma_{21}}\rho_{12}^{*} & 0 & \gamma_{21}\rho_{22} \end{pmatrix} \tag{3.3.50}$$

Since the Choi matrix associated to

$$\Lambda^{(3)}_{\Gamma(\gamma_{10},0,\gamma_{21})} \equiv \tilde{\Phi}^{(3)}_{\Gamma(\gamma_{10},0,\gamma_{21})} \circ {\Phi^{(3)}}^{-1}_{\Gamma(\gamma_{10},0,\gamma_{21})}, \tag{3.3.51}$$

is positive semi-definite only if either one of γ_{10}, γ_{21} is set to 0 (and the other is $\leq 1/2$), the channel $\Phi^{(3)}_{\Gamma(\gamma_{10}\neq 0,0,\gamma_{21}\neq 0)}$ is never degradable.

Degradability for $\gamma_{21} = 0$

The output state of $\Phi^{(3)}_{\Gamma(\gamma_{10},\gamma_{20},0)}$ is:

$$\Phi^{(3)}_{\Gamma(\gamma_{10},\gamma_{20},0)}(\rho) = \begin{pmatrix} \gamma_{10}\rho_{11} + \gamma_{20}\rho_{22} + \rho_{00} & \sqrt{1-\gamma_{10}}\rho_{01} & \sqrt{1-\gamma_{20}}\rho_{02} \\ \sqrt{1-\gamma_{10}}\rho^*_{01} & (1-\gamma_{10})\,\rho_{11} & \sqrt{1-\gamma_{10}}\sqrt{1-\gamma_{20}}\rho_{12} \\ \sqrt{1-\gamma_{20}}\rho^*_{02} & \sqrt{1-\gamma_{10}}\sqrt{1-\gamma_{20}}\rho^*_{12} & (1-\gamma_{20})\,\rho_{22} \end{pmatrix} \tag{3.3.52}$$

While the state of the environment is:

$$\tilde{\Phi}^{(3)}_{\Gamma(\gamma_{10},\gamma_{20},0)}(\rho) = \begin{pmatrix} (1-\gamma_{10})\,\rho_{11} + (1-\gamma_{20})\,\rho_{22} + \rho_{00} & \sqrt{\gamma_{10}}\rho_{01} & \sqrt{\gamma_{20}}\rho_{02} \\ \sqrt{\gamma_{10}}\rho^*_{01} & \gamma_{10}\rho_{11} & \sqrt{\gamma_{10}}\sqrt{\gamma_{20}}\rho_{12} \\ \sqrt{\gamma_{20}}\rho^*_{02} & \sqrt{\gamma_{10}}\sqrt{\gamma_{20}}\rho^*_{12} & \gamma_{20}\rho_{22} \end{pmatrix} \tag{3.3.53}$$

Given the degrading map

$$\Lambda^{(3)}_{\Gamma(\gamma_{10},\gamma_{20},0)} \equiv \tilde{\Phi}^{(3)}_{\Gamma(\gamma_{10},\gamma_{20},0)} \circ {\Phi^{(3)}}^{-1}_{\Gamma(\gamma_{10},\gamma_{20},0)}, \tag{3.3.54}$$

checking the positivity of the associated Choi matrix yields the degradability condition:

$$\gamma_{10} \leq \frac{1}{2} \wedge \gamma_{20} \leq \frac{1}{2} \tag{3.3.55}$$

Degradability conditions

Compounding the results exposed in this Subsection, the degradability conditions for $\Phi^{(3)}_{\Gamma(\gamma_{10},\gamma_{20},\gamma_{21})}$ are found:

$$\begin{gathered} \Phi^{(3)}_{\Gamma(\gamma_{10},\gamma_{20},\gamma_{21})} \text{ is degradable} \\ \Uparrow \\ \left(\gamma_{10} = 0 \wedge \gamma_{20} + \gamma_{21} \leq \frac{1}{2}\right) \vee \left(\gamma_{21} = 0 \wedge \gamma_{10} \leq \frac{1}{2} \wedge \gamma_{20} \leq \frac{1}{2}\right) \end{gathered} \tag{3.3.56}$$

The conditions in (3.3.56) are illustrated in Figure 3.3.2.

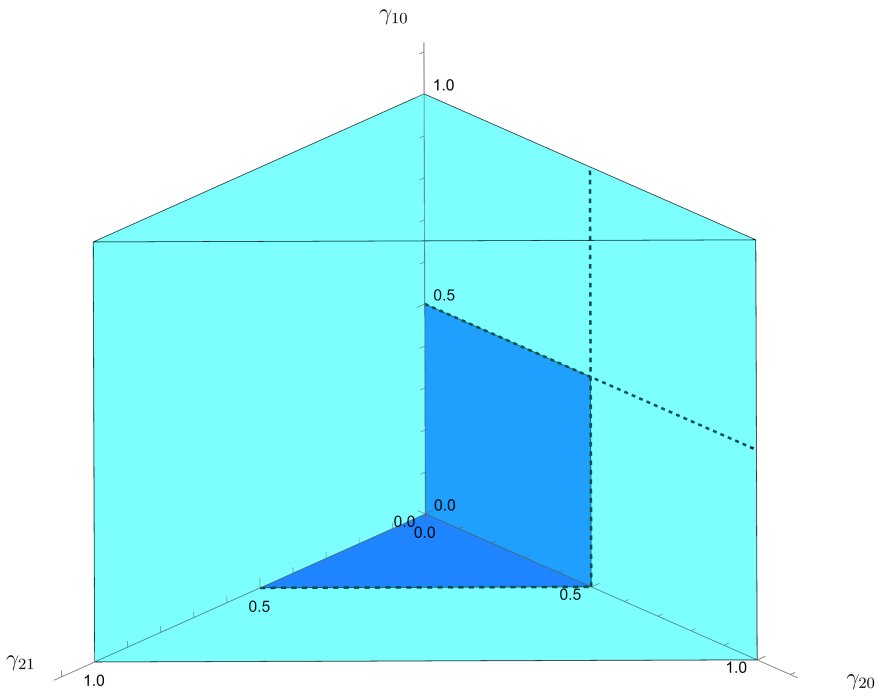

Figure 3.3.2: The plot is cast in the parameter space for a 3-dimensional MAD channel; all these channels satisfy the conditions (3.3.10), which are represented in cyan in the plot, while the blue regions correspond to the degradability conditions reported in (3.3.57)

Additional degradable settings

One may wonder if the conditions in (3.3.56) encompass all the degradability regions for $\Phi^{(3)}_{\Gamma(\gamma_{10},\gamma_{20},\gamma_{21})}$; particularly, it is not clear whether there exists a configuration of $\{\gamma_{10},\gamma_{20},\gamma_{21}\}$ such that $\gamma_{10},\gamma_{20},\gamma_{21} \neq 0$ and $\Phi^{(3)}_{\Gamma(\gamma_{10},\gamma_{20},\gamma_{21})}$ is degradable. To tackle this question, it is possible to exploit the result in (4.4.2), which states that the channel forming an arbitrary decomposition of a degradable channel must be degradable themselves. The right-most channel in the decomposition (3.3.30) of a generic 3-dimensional MAD channel is only degradable if either one of γ_{10},γ_{21} is set to 0, therefore it is not possible to find a configuration $\{\gamma_{10},\gamma_{20},\gamma_{21}\}$ such that $\gamma_{10},\gamma_{20},\gamma_{21} \neq 0$ and $\Phi^{(3)}_{\Gamma(\gamma_{10},\gamma_{20},\gamma_{21})}$ is degradable. Thus, (3.3.56) can be rewritten in a more strict form:

$$\begin{gathered}\Phi^{(3)}_{\Gamma(\gamma_{10},\gamma_{20},\gamma_{21})} \text{ is degradable} \\ \Updownarrow \\ \left(\gamma_{10}=0 \wedge \gamma_{20}+\gamma_{21} \leq \frac{1}{2}\right) \vee \left(\gamma_{21}=0 \wedge \gamma_{10} \leq \frac{1}{2} \wedge \gamma_{20} \leq \frac{1}{2}\right)\end{gathered} \tag{3.3.57}$$

Note that this means that in the case of 3-dimensional MAD channels, the condition $\operatorname{rank}\left(\Phi^{(3)}_{\Gamma}(\rho)\right) \geq \operatorname{rank}\left(\tilde{\Phi}^{(3)}_{\Gamma}(\rho)\right)\ \forall\rho$ is a necessary condition for the degradability of

$\Phi_{\Gamma}^{(3)}$; this is not true in general, a counterexample for 4-dimensional MAD's is offered in **??**.

3.3.j Quantum capacity of single decay 3-dimensional MAD channel

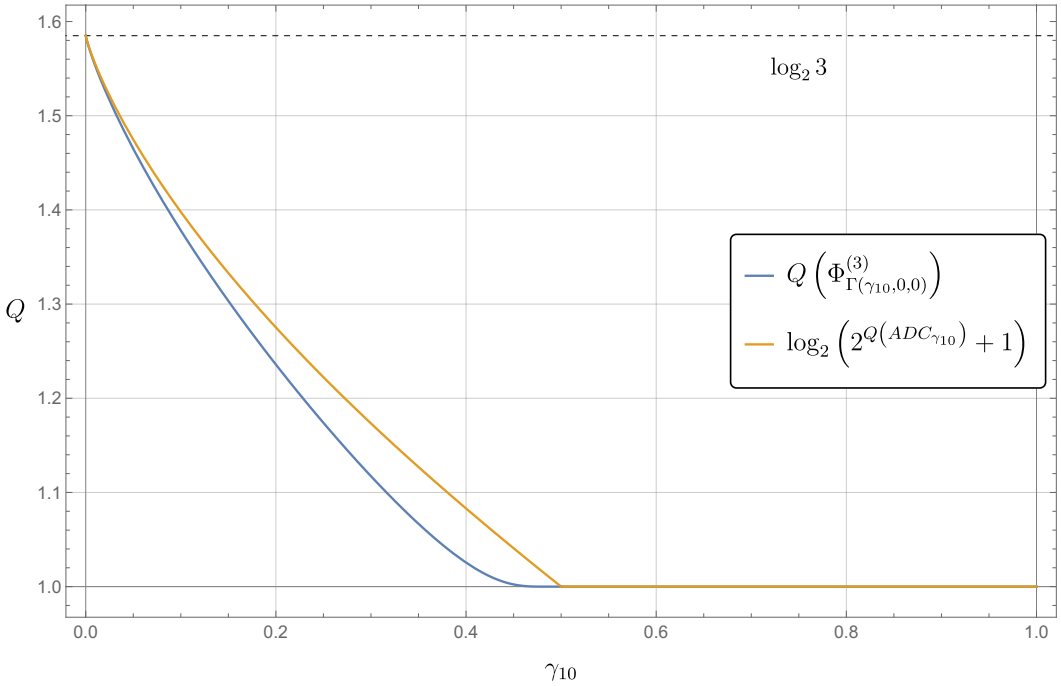

Figure 3.3.3: The quantum capacity of a single decay 3-dimensional MAD channel in plotted here in blue, while the upper bound corresponding to (3.2.4) is plotted in orange.

Consider the channel $\Phi^{(3)}_{\Gamma(\gamma_{10},0,0)}$; as a consequence of the findings in 3.3.f, the capacity functionals of this channel are the same as those of the other single decay 3-dimensional MAD's. Furthermore, according to (3.3.57), the channel is degradable if and only if $0 \leq \gamma_{10} \leq 1/2$. This channel exhibits the PCDS structure [CG21b] (3.2.1), where Φ_{AA} corresponds to the amplitude damping channel $ADC_{\gamma_{10}}$ and $\Phi_{\mathrm{BB}} = \mathbb{1}_{\mathrm{BB}}$, a property that will become useful in the analysis of its quantum capacity. For the degradable region $0 \leq \gamma_{10} \leq 1/2$, the quantum capacity of the channel $Q\left(\Phi^{(3)}_{\Gamma(\gamma_{10},0,0)}\right)$ can be computed using (3.3.41); at $\gamma_{10} = 1/2$, $ADC_{\gamma_{10}}$ is degradable and has null capacity, thus (3.2.6) holds:

$$Q\left(\Phi^{(3)}_{\Gamma(\gamma_{10}=1/2,0,0)}\right) = 1 \tag{3.3.58}$$

Additionally, since the channel presents a noiseless subspace spanned by $\{|0\rangle, |1\rangle\}$, 1 is also a lower bound for the quantum capacity of $\Phi^{(3)}_{\Gamma(\gamma_{10},0,0)}$:

$$Q\left(\Phi^{(3)}_{\Gamma(\gamma_{10},0,0)}\right) \geq 1. \tag{3.3.59}$$

Hence, combining (3.3.59), (3.3.58) and the monotonicity properties (3.3.40):

$$Q\left(\Phi^{(3)}_{\Gamma(\gamma_{10},0,0)}\right) = 1 \quad \forall\, \frac{1}{2} \leq \gamma_{10} \leq 1 \tag{3.3.60}$$

The computations for the quantum capacity of a single decay 3-dimensional MAD channel are plotted in Figure 3.3.3.

4

Properties of MAD channels and 4-dimensional MAD channels

This chapter will focus on the exposition of some general properties of Multi-Level Amplitude Damping channels that were found during this work of thesis. Most of these properties hold for any dimension d, potentially allowing future studies of MAD channels in higher dimensions to be built upon these results.

4.1 Settings for d-dimensional MAD channels

The settings for d-dimensional MAD channels have already been defined in Subsection 3.3.a. The relation (3.3.5), in particular, will turn out to be extremely useful in Section 4.2 for the derivation of the composition rules of MAD channels.

Settings for 4-dimensional MAD channels

Substituting $d = 4$ in the definitions given in 3.3.a, one obtains the settings that describe a 4-dimensional MAD channel $\Phi_{\Gamma}^{(4)}$, which is completely identified by the transition

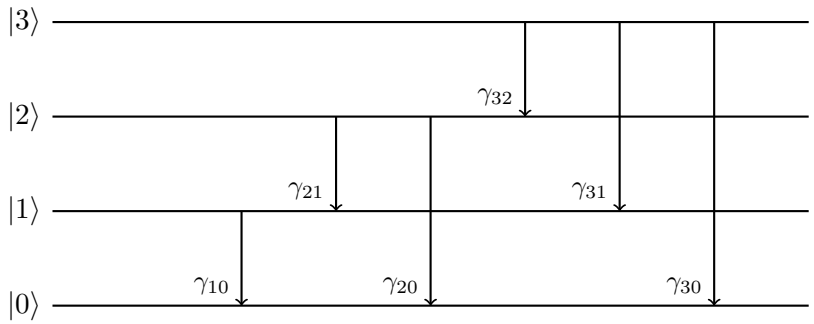

Figure 4.1.1: MAD channels represent decay processes, where each level of a system has a fixed probability of decaying onto a lower level. Here, a schematic depiction of a 4-dimensional MAD is reported

matrix Γ:

$$\Gamma \equiv \begin{pmatrix} 1 & 0 & 0 & 0 \\ \gamma_{10} & 1-\gamma_{10} & 0 & 0 \\ \gamma_{20} & \gamma_{21} & 1-\gamma_{20}-\gamma_{21} & 0 \\ \gamma_{30} & \gamma_{31} & \gamma_{32} & 1-\gamma_{30}-\gamma_{31}-\gamma_{32} \end{pmatrix}, \tag{4.1.1}$$

whose elements satisfy are real, ≥ 0 and ≤ 1, accordingly to (3.3.3). The Kraus set of $\Phi_\Gamma^{(4)}$ is composed by the Kraus operators:

$$K_{00} = \begin{pmatrix} 1 & 0 & 0 & 0 \\ 0 & \sqrt{1-\gamma_{10}} & 0 & 0 \\ 0 & 0 & \sqrt{1-\gamma_{20}-\gamma_{21}} & 0 \\ 0 & 0 & 0 & \sqrt{1-\gamma_{30}-\gamma_{31}-\gamma_{32}} \end{pmatrix}$$

$$K_{01} = \begin{pmatrix} 0 & \sqrt{\gamma_{10}} & 0 & 0 \\ 0 & 0 & 0 & 0 \\ 0 & 0 & 0 & 0 \\ 0 & 0 & 0 & 0 \end{pmatrix} K_{02} = \begin{pmatrix} 0 & 0 & \sqrt{\gamma_{20}} & 0 \\ 0 & 0 & 0 & 0 \\ 0 & 0 & 0 & 0 \\ 0 & 0 & 0 & 0 \end{pmatrix} K_{12} = \begin{pmatrix} 0 & 0 & 0 & 0 \\ 0 & 0 & \sqrt{\gamma_{21}} & 0 \\ 0 & 0 & 0 & 0 \\ 0 & 0 & 0 & 0 \end{pmatrix} \tag{4.1.2}$$

$$K_{03} = \begin{pmatrix} 0 & 0 & 0 & \sqrt{\gamma_{30}} \\ 0 & 0 & 0 & 0 \\ 0 & 0 & 0 & 0 \\ 0 & 0 & 0 & 0 \end{pmatrix} K_{13} = \begin{pmatrix} 0 & 0 & 0 & 0 \\ 0 & 0 & 0 & \sqrt{\gamma_{31}} \\ 0 & 0 & 0 & 0 \\ 0 & 0 & 0 & 0 \end{pmatrix} K_{23} = \begin{pmatrix} 0 & 0 & 0 & 0 \\ 0 & 0 & 0 & 0 \\ 0 & 0 & 0 & \sqrt{\gamma_{32}} \\ 0 & 0 & 0 & 0 \end{pmatrix}$$

Given a generic input $\rho \in \sigma(\mathcal{H}_4)$:

$$\rho \equiv \begin{pmatrix} \rho_{00} & \rho_{01} & \rho_{02} & \rho_{03} \\ \rho_{01}* & \rho_{11} & \rho_{12} & \rho_{13} \\ \rho_{02}^* & \rho_{12}^* & \rho_{22} & \rho_{23} \\ \rho_{03}^* & \rho_{13}^* & \rho_{23}^* & \rho_{33} \end{pmatrix}, \tag{4.1.3}$$

the corresponding output state of the channel $\Phi_\Gamma^{(4)}$ is:

$$\Phi_\Gamma^{(4)}(\rho) = \begin{pmatrix} \rho_{00}+\gamma_{10}\rho_{11}+\gamma_{20}\rho_{22}+\gamma_{30}\rho_{33} & \sqrt{1-\gamma_{10}}\rho_{01} & \sqrt{1-\gamma_{20}-\gamma_{21}}\rho_{02} & \sqrt{1-\gamma_{30}-\gamma_{31}-\gamma_{32}}\rho_{03} \\ \rho_{01}^*\sqrt{1-\gamma_{10}} & (1-\gamma_{10})\rho_{11}+\gamma_{21}\rho_{22}+\gamma_{31}\rho_{33} & \sqrt{1-\gamma_{10}}\sqrt{1-\gamma_{20}-\gamma_{21}}\rho_{12} & \sqrt{1-\gamma_{10}}\sqrt{1-\gamma_{30}-\gamma_{31}-\gamma_{32}}\rho_{13} \\ \rho_{02}^*\sqrt{1-\gamma_{20}-\gamma_{21}} & \rho_{12}^*\sqrt{1-\gamma_{10}}\sqrt{1-\gamma_{20}-\gamma_{21}} & (1-\gamma_{20}-\gamma_{21})\rho_{22}+\gamma_{32}\rho_{33} & \sqrt{1-\gamma_{20}-\gamma_{21}}\sqrt{1-\gamma_{30}-\gamma_{31}-\gamma_{32}}\rho_{23} \\ \rho_{03}^*\sqrt{1-\gamma_{30}-\gamma_{31}-\gamma_{32}} & \rho_{13}^*\sqrt{1-\gamma_{10}}\sqrt{1-\gamma_{30}-\gamma_{31}-\gamma_{32}} & \rho_{23}^*\sqrt{1-\gamma_{20}-\gamma_{21}}\sqrt{1-\gamma_{30}-\gamma_{31}-\gamma_{32}} & (1-\gamma_{30}-\gamma_{31}-\gamma_{32})\rho_{33} \end{pmatrix} \tag{4.1.4}$$

while the output state of the complementary channel $\tilde{\Phi}_\Gamma^{(4)}$ is given in TODO. Refer to Figure 4.1.1 for a schematic representation of 4-dimensional MAD channels.

4.2 Composition of MAD channels

As seen in **??** and **??**, MAD channels in $d = 2$ (ADC's) and $d = 3$ are closed under composition, meaning that the composition of two d-dimensional MAD channels for $d = 2, 3$ is still a d-dimensional MAD channel, whose transition probabilities can be found and depend on the transition probabilities of the starting channels. In this section, a general rule for the composition of d-dimensional will be derived. The closeness of

these channels under composition will be first assumed and then verified *a posteriori* using the composition rules that were found. First, one needs to define three transition matrices $\Gamma, \Gamma', \Gamma''$, whose transition probabilities are, respectively, $\gamma_{ji}, \gamma'_{ji}, \gamma''_{ji}$; then, one reminds that, substituting (3.3.1) into (2.4.4), MAD channels assume the form:

$$\Phi_\Gamma(\rho) = \sum_{i=0}^{j-1}\sum_{j=1}^{d-1} \gamma_{ji}\rho_{jj}\,|i\rangle\langle i| + \sum_{i=0}^{d-1}\sum_{j=1}^{d-1} \sqrt{\gamma_{ii}\gamma_{jj}}\rho_{ij}\,|i\rangle\langle j|\,. \tag{4.2.1}$$

One may try to write:

$$\Phi_\Gamma = \Phi_{\Gamma''} \circ \Phi_{\Gamma'} \tag{4.2.2}$$

and try to find a function f such that:

$$\Gamma = f\left(\Gamma', \Gamma''\right). \tag{4.2.3}$$

If one were to write $\Phi_{\Gamma''} \circ \Phi_{\Gamma'}(\rho)$ in the form (4.2.1), they would obtain:

$$\begin{aligned}\Phi_{\Gamma''} \circ \Phi_{\Gamma'}(\rho) = &\sum_{i=0}^{l-1}\sum_{l=1}^{j-1}\sum_{j=1}^{d-1} \gamma''_{li}\gamma'_{jl}\rho_{jj}\,|i\rangle\langle i| + \\ &\sum_{i=0}^{j-1}\sum_{j=1}^{d-1} \gamma''_{ii}\gamma'_{ji}\rho_{jj}\,|i\rangle\langle i| + \\ &\sum_{i=0}^{j-1}\sum_{j=1}^{d-1} \gamma''_{ji}\gamma'_{jj}\rho_{jj}\,|i\rangle\langle i| + \\ &\sum_{i=0}^{d-1}\sum_{j=1}^{d-1} \sqrt{\gamma''_{ii}\gamma'_{ii}\gamma''_{jj}\gamma'_{jj}}\rho_{ij}\,|i\rangle\langle j|\,,\end{aligned} \tag{4.2.4}$$

which, employing the last property in (3.3.3), translates to

$$\Phi_{\Gamma''} \circ \Phi_{\Gamma'}(\rho) = \sum_{i=0}^{j-1}\sum_{j=1}^{d-1}\left(\sum_{l=0}^{d-1} \gamma''_{li}\gamma'_{jl}\right)\rho_{jj}\,|i\rangle\langle i| + \sum_{i=0}^{d-1}\sum_{j=1}^{d-1} \sqrt{\gamma''_{ii}\gamma'_{ii}\gamma''_{jj}\gamma'_{jj}}\rho_{ij}\,|i\rangle\langle j| \tag{4.2.5}$$

This would represent the right hand side of (4.2.2) for a generic input ρ. By direct computation, it is possible to verify that fixing the composition laws:

$$\gamma_{ji} = \sum_{l=0}^{d-1} \gamma''_{li}\gamma'_{jl} \quad \forall i \leq j \tag{4.2.6}$$

reduces (4.2.5) to (4.2.1). Therefore, it is possible to infer that the composition of two d-dimensional MAD channels is a d-dimensional MAD channel, whose transition probabilities depend on those of the initial channels as in (4.2.6). In terms of transition matrices, (4.2.6) can easily be obtained by setting $f\left(\Gamma', \Gamma''\right) \equiv \Gamma'\Gamma''$ in (4.2.3), so that the composition rules of MAD channels can be summarized by:

$$\begin{aligned}\Phi_\Gamma &= \Phi_{\Gamma''} \circ \Phi_{\Gamma'} \\ \Gamma &= \Gamma'\Gamma''\end{aligned} \tag{4.2.7}$$

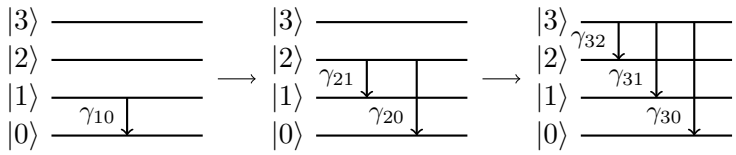

Figure 4.2.1: Visual representation of the decomposition of a 4-dimensional MAD channel using (4.2.11), read from left to right in "chronological" order.

4.2.a Useful decompositions of MAD channels

Following (4.2.7), one could find various decompositions of a generic MAD channels which may help to simplify the process of finding the capacity of the channel. In this section, the most intuitive decompositions will be listed.

Separated decays from increasing levels

This decomposition is the easiest to derive and also the most useful; it is found by defining the matrices:

$$\begin{aligned}\Gamma_k &\equiv \mathbb{1}_d + \sum_{i=0}^{k-1} \gamma_{ki} \left|k\right\rangle\!\left\langle i\right| - \sum_{i=0}^{k-1} \gamma_{ki} \left|k\right\rangle\!\left\langle k\right| \\ \Gamma^{(k)} &\equiv \mathbb{1}_d + \sum_{j=1}^{k-1}\sum_{i=0}^{j-1} \gamma_{ji} \left|j\right\rangle\!\left\langle i\right| - \sum_{j=1}^{k-1}\sum_{i=0}^{j-1} \gamma_{ji} \left|j\right\rangle\!\left\langle j\right|,\end{aligned} \tag{4.2.8}$$

where $k < d$ and Γ_k represents a special kind of MAD channel where only the level $|k\rangle$ is allowed to decay, while $\Gamma^{(k)}$ represents a MAD channel where the decays from levels $|k\rangle$ and upwards are forbidden. In this setting, the most generic d-dimensional transition matrix Γ in (3.3.4) is equal to $\Gamma^{(d)}$. By direct computation, setting $k = d-1$ in (4.2.8) leads to:

$$\Gamma^{(d)} = \Gamma^{(d-1)}\Gamma_{d-1}, \tag{4.2.9}$$

then, by iterating (4.2.9), one arrives at the decomposition:

$$\Gamma = \Gamma^{(d)} = \Gamma_1\Gamma_2 ... \Gamma_{d-1} \tag{4.2.10}$$

which, by employing (4.2.7), translates to:

$$\Phi_\Gamma = \Phi_{\Gamma_{d-1}} \circ ... \circ \Phi_{\Gamma_1}. \tag{4.2.11}$$

Intuitively speaking, (4.2.11) means that in a MAD channel, the lower energy levels "have precedence" when decaying, as represented in Figure 4.2.1.

The matrices Γ_k can be decomposed even further: one needs to define the matrices:

$$\begin{aligned}
\Gamma_k^{(n)} &\equiv \mathbb{1}_d + \gamma'_{kn} |k\rangle\langle n| - \gamma'_{kn} |k\rangle\langle k| \\
T_k^{(n)} &\equiv \mathbb{1}_d + \sum_{\substack{i=0 \\ i\neq n}}^{k-1} \gamma_{ki} |k\rangle\langle i| - \sum_{\substack{i=0 \\ i\neq n}}^{k-1} \gamma_{ki} |k\rangle\langle k| \\
T_k^{(n)} &= \Gamma_k - \gamma_{kn} |k\rangle\langle n| + \gamma_{kn} |k\rangle\langle k|
\end{aligned} \tag{4.2.12}$$

where $n < k$; this matrices compose in the following way:

$$\begin{aligned}
\gamma'_{kn} &\equiv \gamma_{kn} \left(1 - \sum_{\substack{i=0 \\ i\neq n}}^{k-1} \gamma_{ki} \right)^{-1} \\
\Gamma_k &= T_k^{(n)} \Gamma_k^{(n)}
\end{aligned} \tag{4.2.13}$$

The physical interpretation is clear: in this setting, given the decays from the level $|k\rangle$, the decay onto the level $|n\rangle$ needs to be performed at the end of the process. In order to achieve this, one needs to modify the amplitude γ_{kn} as in (4.2.13); note that the denominator of γ'_{kn} in (4.2.13) does not depend on γ_{kn}.

MAD channel as composition of single decays

One may want to expand on the idea behind (4.2.13) in order to create a composition of single transition matrices. This can be achieved by a slight redefinition of the matrices in (**??**):

$$\begin{aligned}
\Xi_k^{(n)} &\equiv \mathbb{1}_d + \gamma_{kn}^{(n+1)} |k\rangle\langle n| - \gamma_{kn}^{(n+1)} |k\rangle\langle k| \\
H_k^{(n)} &\equiv \mathbb{1}_d + \sum_{i=n}^{k-1} \gamma_{ki} |k\rangle\langle i| - \sum_{i=n}^{k-1} \gamma_{ki} |k\rangle\langle k|
\end{aligned} \tag{4.2.14}$$

where $n < k$. The $\Xi_k^{(n)}$'s represent single decay MAD channels with modified amplitudes w.r.t. the original channel, while the $H_k^{(n)}$'s represent MAD channels where only the $|k\rangle$ level can decay, with the same amplitudes as the original channel and having the transitions onto the lowest n levels forbidden. One can verify that:

$$H_k^{(0)} = \Gamma_k \tag{4.2.15}$$

which matches the descriptive definition given above. In order to find the values of $\gamma_{kn}^{(n+1)}$ in terms of the original amplitudes, one must try to solve the iterative equation:

$$H_k^{(n)} = H_k^{(n+1)} \Xi_k^{(n)} \tag{4.2.16}$$

The (4.2.16) fixes the values of $\gamma_{kn}^{(n+1)}$:

$$\gamma_{kn}^{(n+1)} \equiv \frac{\gamma_{kn}}{1 - \sum_{i=n+1}^{k-1} \gamma_{ki}} \tag{4.2.17}$$

which also implies that:

$$H_k^{(k-1)} = \Xi_k^{(k-1)} \tag{4.2.18}$$

Using the iterative (4.2.16) and employing (4.2.15), (4.2.18) allows for the decomposition of Γ_k in single level transition matrices:

$$\begin{aligned} \Gamma_k &= H^{(0)} \\ &= H_k^{(1)} \Xi_k^{(0)} \\ &= H_k^{(2)} \Xi_k^{(1)} \Xi_k^{(0)} \\ &\dots \\ &= \Xi_k^{(k-1)} \dots \Xi_k^{(0)} \end{aligned} \tag{4.2.19}$$

Combining (4.2.10) and (4.2.19), it is possible to consider a generic MAD channel as a composition of single-decay MAD channels, with appropriately modified amplitudes:

$$\Gamma = \prod_{\substack{k=1 \\ \rightarrow}}^{d-1} \left(\Xi_k^{(k-1)} \dots \Xi_k^{(0)} \right) \tag{4.2.20}$$

where $\prod_{\rightarrow}$ indicates that the product is meant to be expanded from left to right for increasing k's. The (4.2.20) translates to:

$$\Phi_\Gamma = \bigodot_{\substack{k=1 \\ \leftarrow}}^{d-1} \left(\Phi_{\Xi_k^{(0)}} \circ \dots \circ \Phi_{\Xi_k^{(k-1)}} \right) \tag{4.2.21}$$

where $\bigodot_{\leftarrow}$ indicates a composition of channels that is meant to be expanded from right to left for increasing k's.

Separated decays onto increasing levels

TODO maybe.

4.3 Equivalence of single decay MAD channels

Expanding on the ideas introduced in Subsection 3.3.f, it is possible to prove that the capacity functionals of any single decay d-dimensional MAD channel only depend on the single transition probability, not on the levels involved in the decay. Consider the swap unitaries:

$$U_{mn} \equiv \mathbb{1}_{\mathcal{H}_d} - |m\rangle\langle m| - |n\rangle\langle n| + |m\rangle\langle n| + |n\rangle\langle m| \quad m, n \in \{0, \dots, d-1\}, \tag{4.3.1}$$

and the associated unitary quantum channels:

$$\mathcal{U}_{mn}(\bullet) \equiv U_{mn} \bullet U_{mn}; \tag{4.3.2}$$

note that, if $m = n$, then $\mathcal{U}_{mn} = \mathbb{1}_{\sigma(\mathcal{H}_d)}$. Let $\Gamma_{ji}(\gamma)$, $j > i$, be a single decay transition matrix of transition probability γ:

$$\Gamma_{ji}(\gamma) \equiv \mathbb{1}_{\mathcal{H}_d} + \gamma\,|j\rangle\langle i| - \gamma\,|j\rangle\langle j|\,, \tag{4.3.3}$$

It can be shown that:

$$\begin{aligned} \mathcal{U}_{kj} \circ \Phi_{\Gamma_{ji}(\gamma)} \circ \mathcal{U}_{kj} &= \Phi_{\Gamma_{ki}(\gamma)} \quad k > i \\ \mathcal{U}_{ki} \circ \Phi_{\Gamma_{ji}(\gamma)} \circ \mathcal{U}_{ki} &= \Phi_{\Gamma_{jk}(\gamma)} \quad k < j \end{aligned} \tag{4.3.4}$$

Utilizing the relations (4.3.4), it is possible to transform $\Phi_{\Gamma_{ji}(\gamma)}$ into another single decay MAD channel $\Phi_{\Gamma_{j'i'}(\gamma)}$, $j' > i'$. In order to achieve this, one needs to distinguish the two cases where $j' \geq j$ or $j' < j$:

$$\begin{aligned} j' \geq j \Rightarrow \Phi_{\Gamma_{j'i'}(\gamma)} &= \mathcal{U}_{i'i} \circ \mathcal{U}_{j'j} \circ \Phi_{\Gamma_{ji}(\gamma)} \circ \mathcal{U}_{j'j} \circ \mathcal{U}_{i'i} \\ j' < j \Rightarrow \Phi_{\Gamma_{j'i'}(\gamma)} &= \mathcal{U}_{j'j} \circ \mathcal{U}_{i'i} \circ \Phi_{\Gamma_{ji}(\gamma)} \circ \mathcal{U}_{i'i} \circ \mathcal{U}_{j'j} \end{aligned} \tag{4.3.5}$$

Employing (4.3.5) and the pipeline inequalities (**??**), one can conclude that the capacity functionals of single decay MAD channels depend only on their transition probability, not on the levels involved in the decay.

4.4 Composition of degradable channels

The topic of this section is not strictly related to MAD channels; however, its usefulness in the derivation of the degradability zone of MAD's will become apparent in section 4.6. Given two LCPT maps Ψ_1, Ψ_2 and their composition $\Psi \equiv \Psi_2 \circ \Psi_1$, it will be shown that:

$$\begin{gathered} \Psi = \Psi_2 \circ \Psi_1 \\ \Psi \text{ degradable} \Rightarrow \Psi_1, \Psi_2 \text{ degradable} \end{gathered} \tag{4.4.1}$$

Or, more eloquently:

$$\begin{gathered} \Psi = \Psi_2 \circ \Psi_1 \\ \exists\,\Lambda \text{ LCPT} : \Lambda \circ \Psi = \tilde{\Psi} \Rightarrow \begin{cases} \exists\,\Lambda_1 \text{ LCPT} : \Lambda_1 \circ \Psi_1 = \tilde{\Psi}_1 \\ \exists\,\Lambda_2 \text{ LCPT} : \Lambda_2 \circ \Psi_2 = \tilde{\Psi}_2 \end{cases} \end{gathered} \tag{4.4.2}$$

Complementary channels equivalence

The complementary channel $\tilde{\Psi}$ is unitarily equivalent to its counterpart written in terms of the channels $\Psi_{1,2}$:

$$\tilde{\Psi}'(\rho) = \tilde{\Psi}_1(\rho)_{E1} \otimes \tilde{\Psi}_2\left(\Psi_1(\rho)\right)_{E2}, \tag{4.4.3}$$

i.e. the output of the complementary channel of Ψ, in this representation, corresponds to the tensor product of two environment states in the systems $E1, E2$. By (2.5.4), there must exist a unitary transformation $\mathfrak{V}$ such that:

$$\tilde{\Psi}'(\rho) = \mathfrak{V}\left(\tilde{\Psi}(\rho)\right) = V\tilde{\Psi}(\rho)V^{\dagger}. \tag{4.4.4}$$

Ψ_2 is degradable

Define $\rho_1 \equiv \Psi_1(\rho)$; using this definition, the degradability hypothesis of Ψ reads:

$$\tilde{\Psi}(\rho) = \Lambda \circ \Psi_2(\rho_1). \tag{4.4.5}$$

One can then build the LCPT channel Ω_2:

$$\Omega_2 \equiv \mathrm{tr}_{E1} \circ \mathfrak{V}, \tag{4.4.6}$$

where tr_{E1} is the LCPT channel describing the partial trace over the $E1$ environment. Applying Ω_2 to (4.4.5) leads to:

$$\tilde{\Psi}_2\left(\rho_1\right) = \Omega_2 \circ \Lambda \circ \Psi_2(\rho_1) \tag{4.4.7}$$

Therefore, if one thought of Ψ_1 as a state preparation device, by defining the LCPT $\Lambda_2 \equiv \Omega_2 \circ \Lambda$ one would obtain:

$$\tilde{\Psi}_2 = \Lambda_2 \circ \Psi_2 \tag{4.4.8}$$

proving the degradability of Φ_2.

Ψ_1 is degradable

Define the LCPT map:

$$\Omega_1 \equiv \mathrm{tr}_{E2} \circ \mathfrak{V} \tag{4.4.9}$$

Starting from $\tilde{\Psi} = \Lambda \circ \Psi$, apply Ω_1 to both sides, which yields:

$$\tilde{\Psi}_1 = \Omega_1 \circ \Lambda \circ \Psi_2 \circ \Psi_1. \tag{4.4.10}$$

Then, one could define the LCPT

$$\Lambda_1 = \Omega_1 \circ \Lambda \circ \Psi_2 \tag{4.4.11}$$

which can be substituted into (4.4.10):

$$\tilde{\Psi}_1 = \Lambda_1 \circ \Psi_1. \tag{4.4.12}$$

(4.4.12) and (4.4.8) together prove (4.4.2).

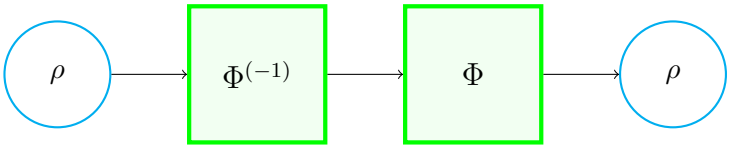

Figure 4.5.1: The map $\Phi^{(-1)}$ acts as the right inverse of the MAD channel Φ

4.5 Inverse maps of MAD channels

It is not always possible to find the (left or right) inverse map of a LCPT channel, a clear example of this fact are the channels which send a D-dimensional system into a d-dimensional system, where $d < D$. This is not the case for MAD channels; in fact it turns out that their inverse maps has a rather intuitive, albeit convoluted, definition. In the following, the right inverse map (represented in Figure 4.5.1) of a generic MAD channel will be derived.

4.5.a Inverse maps of ADC's

The inverse map of an ADC provides a valuable guide for the derivation of the inverse of a MAD channel. The reader can find the definition of the ADC's in **??**. The scope of this subsection is to find the right inverse map of an ADC:

$$\begin{gathered} A_\gamma^{-1} : \sigma\left(\mathcal{H}_2\right) \mapsto \sigma\left(\mathcal{H}_2\right) \\ A_\gamma \circ A_\gamma^{-1}(\rho) = \rho \end{gathered} \tag{4.5.1}$$

The map A_γ^{-1}, while trace preserving and linear, is not expected to be completely positive, therefore it is not expected to be a quantum channel. In fact it could be cast in a "pseudo-Kraus" representation:

$$\begin{gathered} A_\gamma^{-1}(\theta) = \tilde{K}_0(\gamma)\theta\tilde{K}_0(\gamma)^\dagger - \tilde{K}_1(\gamma)\theta\tilde{K}_1(\gamma)^\dagger \\ \tilde{K}_0(\gamma) = \begin{pmatrix} 1 & 0 \\ 0 & \frac{1}{\sqrt{1-\gamma}} \end{pmatrix} \quad \tilde{K}_1(\gamma) = \begin{pmatrix} 0 & \sqrt{\frac{\gamma}{1-\gamma}} \\ 0 & 0 \end{pmatrix} \end{gathered} \tag{4.5.2}$$

Notice that, while $\tilde{K}_0(\gamma)$ and $\tilde{K}_1(\gamma)$ form a Kraus set, the "$-$" sign in (4.5.2) implies that A_γ^{-1} is **not** necessarily a quantum channel, as it is not written in the Kraus representation. One could also write (4.5.2) in matrix form:

$$A_\gamma^{-1}(\theta) = \begin{pmatrix} \theta_{00} - \frac{\gamma}{1-\gamma}\theta_{11} & \frac{1}{\sqrt{1-\gamma}}\theta_{01} \\ \frac{1}{\sqrt{1-\gamma}}\theta_{01}^* & \frac{1}{(1-\gamma)}\theta_{11} \end{pmatrix}. \tag{4.5.3}$$

The map defined in (4.5.1) is also the left-inverse of A_γ, which can be verified by direct computation.

4.5.b Inverse of single decay MAD channels

Consider the MAD channel $\Phi_{\Xi_k^{(n)}}$, where $\Xi_k^{(n)}$ is defined in (4.2.14) and the associated transition probability can be found in (4.2.17). This is a single decay MAD channel, which acts on the subspace spanned by $|k\rangle$ and $|n\rangle$ as an ADC with the same transition probability. Therefore, one might be tempted to define the right-inverse of $\Phi_{\Xi_k^{(n)}}$ as the embedding onto $\mathcal{H}_d$ of the right-inverse of an ADC. Let $\Phi^{(-1)}_{\Xi_k^{(n)}}$ be the right inverse of $\Phi_{\Xi_k^{(n)}}$. Given $\theta \in \sigma\left(\text{span}\left\{|k\rangle, |n\rangle\right\}\right)$, $\Phi^{(-1)}_{\Xi_k^{(n)}}$ needs to satisfy:

$$\Phi^{(-1)}_{\Xi_k^{(n)}}(\theta) = \begin{pmatrix} \theta_{nn} - \gamma_{kn}^{(n+1)}\left(1-\gamma_{kn}^{(n+1)}\right)^{-1}\theta_{kk} & \left(1-\gamma_{kn}^{(n+1)}\right)^{-1/2}\theta_{nk} \\ \left(1-\gamma_{kn}^{(n+1)}\right)^{-1/2}\theta_{nk}^{*} & \left(1-\gamma_{kn}^{(n+1)}\right)^{-1}\theta_{kk} \end{pmatrix} \tag{4.5.4}$$

This can be achieved by defining $\Phi^{(-1)}_{\Xi_k^{(n)}}$ as:

$$\Phi^{(-1)}_{\Xi_k^{(n)}}(\rho) \equiv \tilde{K}_0\left(\Xi_k^{(n)}\right)\rho\tilde{K}_0\left(\Xi_k^{(n)}\right)^{\dagger} - \tilde{K}_1\left(\Xi_k^{(n)}\right)\rho\tilde{K}_1\left(\Xi_k^{(n)}\right)^{\dagger}$$

$$\tilde{K}_0\left(\Xi_k^{(n)}\right) \equiv \mathbb{1}_d - \left(1-\left(1-\gamma_{kn}^{(n+1)}\right)^{-1/2}\right)|k\rangle\langle k| \tag{4.5.5}$$

$$\tilde{K}_1\left(\Xi_k^{(n)}\right) \equiv \left(\frac{\gamma_{kn}^{(n+1)}}{1-\gamma_{kn}^{(n+1)}}\right)^{1/2}|n\rangle\langle k|$$

where $\rho \in \sigma\left(\mathcal{H}_d\right)$. It is possible to show, by direct computation, that:

$$\Phi_{\Xi_k^{(n)}} \circ \Phi^{(-1)}_{\Xi_k^{(n)}}(\rho) = \rho \quad \forall \rho \in \sigma\left(\mathcal{H}_d\right) \tag{4.5.6}$$

Notice that the map $\Phi^{(-1)}_{\Xi_k^{(n)}}$ is linear and trace preserving and is also the left-inverse of $\Phi_{\Xi_k^{(n)}}$.

4.5.c Inverse map as composition of inverse maps of single decays

The importance of (4.5.6) lies in the fact that it can be composed to generate the right-inverse map of a general MAD channel. In fact, recall that in (4.2.21) it was shown that a MAD channel can be seen as a composition of single decay MAD channels. Then, by "inverting" those single decay transitions one by one, the resulting channel must be the identity channel. This line of reasoning results in the definition:

$$\Phi_{\Gamma}^{-1} = \bigodot_{\substack{k=1 \\ \rightarrow}}^{d-1}\left(\Phi^{(-1)}_{\Xi_k^{(k-1)}} \circ \ldots \circ \Phi^{(-1)}_{\Xi_k^{(0)}}\right) \tag{4.5.7}$$

which, by construction, satisfies:

$$\Phi_\Gamma \circ \Phi_\Gamma^{-1} = \mathbb{1}. \tag{4.5.8}$$

Since each of the $\Phi^{(-1)}_{\Xi_k^{(n)}}$'s is linear and trace preserving, and a generic composition of such maps holds those same properties, then $\Phi_\Gamma^{(-1)}$ must also be linear and trace preserving.

Notice, finally, that $\Phi_\Gamma^{(-1)}$, again, by construction, is also the left inverse of Φ_Γ.

4.6 Degradability of MAD channels

As seen in **??**, the quantum capacity of degradable channels is computable and corresponds to the maximum (calculated over all possible inputs) of the coherent information **??**. Therefore, it is important to find a complete characterization of the degradability conditions of MAD channels.

Since MAD channels admit a right inverse map, starting from **??**, verifying the degradability of Φ_Γ reduces to verifying that Λ_Γ in:

$$\Lambda_\Gamma \equiv \tilde{\Phi}_\Gamma \circ \Phi_\Gamma^{(-1)} \tag{4.6.1}$$

is LCPT. The map Λ_Γ is linear and trace preserving by construction, while the complete positiveness is not guaranteed; using Choi's theorem **??**, it is possible to verify whether or not Λ_Γ satisfies that last property:

$$\Lambda_\Gamma \text{ is completely positive} \Leftrightarrow C_{\Lambda_\Gamma} \text{ is positive} \tag{4.6.2}$$

where C_{Λ_Γ} is the Choi matrix of the map Λ_Γ, defined as in (2.4.12)[1].

$$\begin{gathered} C_{\Lambda_\Gamma} \equiv \frac{1}{d} \left[\Lambda_\Gamma \otimes \mathbb{1}\right] (|\Omega\rangle\langle\Omega|) \\ |\Omega\rangle\langle\Omega| \text{ maximally entangled state.} \end{gathered} \tag{4.6.3}$$

The computation of the eigenvalues of C_{Λ_Γ} for a generic 4-dimensional Γ turns out to be relatively demanding for a desktop computer (see **??** for details on computation methods), but all degradability regions can be found regardless by means of lateral thinking that simplifies the computation tasks, as demonstrated in 4.7.

4.7 Degradability of 4-dimensional MAD channels

In 3.3.i, the degradability regions for 3-dimensional MAD channels were determined by ensuring that the rank of the output state of the channel was not smaller than the

[1] the factor $1/d$ is kept here for the sake of consistency, but is obviously not necessary when checking for positiveness

rank of the state of the environment (3.3.44), which implied reducing the number of decays in the channel, and checking *a posteriori* whether or not less strict degradability conditions could be found by introducing additional decays to those regions. In the case of 4-dimensional MAD channels $\Phi_\Gamma^{(4)}$, (3.3.44) becomes:

$$\text{rank}\left(\Phi_\Gamma^{(4)}(\rho)\right) \geq \text{rank}\left(\tilde{\Phi}_\Gamma^{(4)}(\rho)\right) \quad \forall\rho, \tag{4.7.1}$$

which implies that the number of decays in the channel needs to not exceed 3. The number of 4-dimensional MAD channels with 3 decays can be found by counting the number of ways one can select 3 different couples (j,i), where $j<i$; the number of such couples is $\binom{4}{2}=6$, which means that the number of 3-decay configurations is $\binom{6}{3}=20$. Many of this configurations are unitarily equivalent and the connecting unitary transformations are of the form (4.3.2); hence, 9 different classes of unitarily different 3-decay channels can be identified. There are also 4 classes of unitarily different 2-decay channels and 1 class of single decay channels. This classes are not identified by the labels on the levels involved in the decays, but rather by the "internal structure" that emerges from the decays.

4.7.a Class 1A

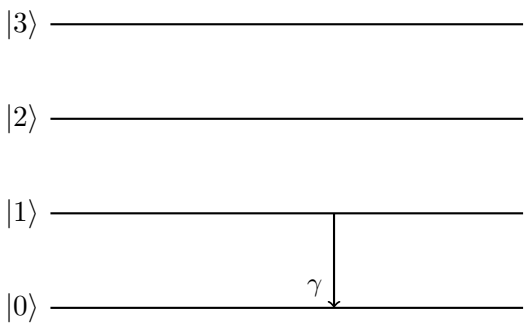

Figure 4.7.1: Class 1A consists of an ADC embedded into the higher dimensional $\mathcal{H}_4$

This class identifies the single decay MAD channels; as seen in Section 4.3, if the transition probability is fixed, all possible configurations of single decay MAD's are unitarily equivalent. Let $\Phi_{\Gamma_{1A}(\gamma)}$ be a generic channel belonging to Class 1A, with transition probability γ. This class presents the PCDS structure (3.2.1), where $\Phi_{BB}=\mathbb{1}_{\sigma(\mathcal{H}_2)}$ and $\Phi_{AA}=ADC_\gamma$ an amplitude damping channel; therefore, following (3.2.2), the degradability conditions of $\Phi_{\Gamma_{1A}(\gamma)}$ are the same as those given in (3.1.15):

$$\Phi_{\Gamma_{1A}(\gamma)} \text{ degradable} \Leftrightarrow \gamma \leq \frac{1}{2}. \tag{4.7.2}$$

The existence of a noiseless subspace guarantees that $\Phi_{\Gamma_{1A}(\gamma)}$ is never antidegradable.

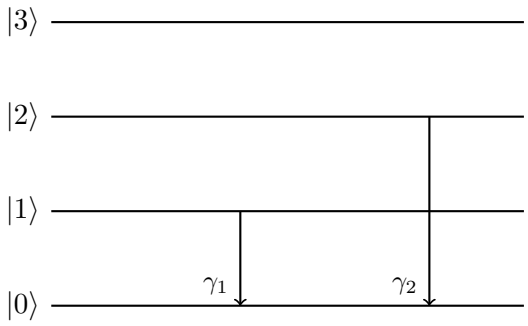

Figure 4.7.2: An example of channel belonging in **Class 2A** is provided by the embedding of $\Phi^{(3)}_{\Gamma(\gamma_1,\gamma_2,0)}$ in $\mathcal{H}_4$.

4.7.b Class 2A

Channels belonging to this class are unitarily equivalent to the MAD channel identified by the transition matrix $\Gamma = \mathbb{1}_{\mathcal{H}_4} + \gamma_1 |1\rangle\langle 0| - \gamma_1 |1\rangle\langle 1| + \gamma_2 |2\rangle\langle 0| - \gamma_2 |2\rangle\langle 2|$, depicted in Figure 4.7.2. Let a generic channel in this class be called $\Phi_{\Gamma_{2A}(\gamma_1,\gamma_2)}$; this channel presents the PCDS structure (3.2.1), where $\Phi_{BB} = \mathbb{1}_{\sigma(\mathcal{H}_1)}$ and $\Phi_{AA} = \Phi^{(3)}_{\Gamma(\gamma_1,\gamma_2,0)}$, where $\Phi^{(3)}_{\Gamma(\gamma_1,\gamma_2,0)}$ is the 3-dimensional MAD channel defined in (3.3.28). Following (3.2.2), the degradability conditions of $\Phi_{\Gamma_{2A}(\gamma_1,\gamma_2)}$ are the same as those given in (3.3.55):

$$\Phi_{\Gamma_{2A}(\gamma_1,\gamma_2)} \text{ degradable} \Leftrightarrow \gamma_1 \leq \frac{1}{2} \wedge \gamma_2 \leq \frac{1}{2} \tag{4.7.3}$$

The existence of a noiseless subspace guarantees that $\Phi_{\Gamma_{2A}(\gamma_1,\gamma_2)}$ is never antidegradable.

4.7.c Class 2B

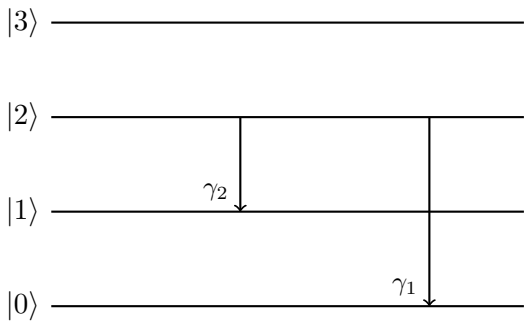

Figure 4.7.3: An example of channel belonging in **Class 2B** is provided by the embedding of $\Phi^{(3)}_{\Gamma(0,\gamma_1,\gamma_2)}$ in $\mathcal{H}_4$.

Channels belonging to this class are unitarily equivalent to the MAD channel identified by the transition matrix $\Gamma = \mathbb{1}_{\mathcal{H}_4} + \gamma_1 |2\rangle\langle 0| + \gamma_2 |2\rangle\langle 1| - (\gamma_1 + \gamma_2) |2\rangle\langle 2|$,

depicted in Figure 4.7.3. Let a generic channel in this class be called $\Phi_{\Gamma_{2B}(\gamma_1,\gamma_2)}$; this channel presents the PCDS structure (3.2.1), where $\Phi_{BB} = \mathbb{1}_{\sigma(\mathcal{H}_1)}$ and $\Phi_{AA} = \Phi^{(3)}_{\Gamma(0,\gamma_1,\gamma_2)}$. Following (3.2.2), the degradability conditions of $\Phi_{\Gamma_{2B}(\gamma_1,\gamma_2)}$ are the same as those given in (3.3.48):

$$\Phi_{\Gamma_{2B}(\gamma_1,\gamma_2)} \text{ degradable} \Leftrightarrow \gamma_1 + \gamma_2 \leq \frac{1}{2} \tag{4.7.4}$$

The existence of a noiseless subspace guarantees that $\Phi_{\Gamma_{2B}(\gamma_1,\gamma_2)}$ is never antidegradable.

4.7.d Class 2C

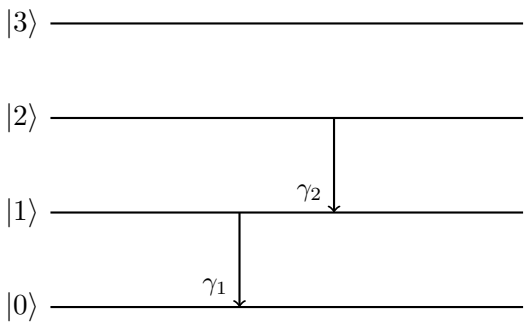

Figure 4.7.4: An example of channel belonging in **Class 2C** is provided by the embedding of $\Phi^{(3)}_{\Gamma(\gamma_1,0,\gamma_2)}$ in $\mathcal{H}_4$.

Channels belonging to this class are unitarily equivalent to the MAD channel identified by the transition matrix $\Gamma = \mathbb{1}_{\mathcal{H}_4} + \gamma_1 |1\rangle\langle 0| - \gamma_1 |1\rangle\langle 1| + \gamma_2 |2\rangle\langle 1| - \gamma_2 |2\rangle\langle 2|$, depicted in Figure 4.7.4. Let a generic channel in this class be called $\Phi_{\Gamma_{2C}(\gamma_1,\gamma_2)}$; this channel presents the PCDS structure (3.2.1), where $\Phi_{BB} = \mathbb{1}_{\sigma(\mathcal{H}_1)}$ and $\Phi_{AA} = \Phi^{(3)}_{\Gamma(\gamma_1,0,\gamma_2)}$. Following (3.2.2) and Subsection 3.3.i, it can be inferred that $\Phi_{\Gamma_{2C}(\gamma_1,\gamma_2)}$ is never degradable The existence of a noiseless subspace guarantees that $\Phi_{\Gamma_{2C}(\gamma_1,\gamma_2)}$ is never antidegradable.

4.7.e Class 2D

Channels belonging to this class are unitarily equivalent to the MAD channel identified by the transition matrix $\Gamma = \mathbb{1}_{\mathcal{H}_4} + \gamma_1 |1\rangle\langle 0| - \gamma_1 |1\rangle\langle 1| + \gamma_2 |3\rangle\langle 2| - \gamma_2 |3\rangle\langle 3|$, depicted in Figure 4.7.4. Let a generic channel in this class be called $\Phi_{\Gamma_{2D}(\gamma_1,\gamma_2)}$; this channel presents the PCDS structure (3.2.1), where $\Phi_{AA} = ADC_{\gamma_1}$ and $\Phi_{BB} = ADC_{\gamma_2}$. Following (3.2.2) and (3.1.15), the degradability conditions of $\Phi_{\Gamma_{2D}(\gamma_1,\gamma_2)}$ are:

$$\Phi_{\Gamma_{2D}(\gamma_1,\gamma_2)} \text{ degradable} \Leftrightarrow \gamma_1 \leq \frac{1}{2} \wedge \gamma_2 \leq \frac{1}{2} \tag{4.7.5}$$

The existence of a noiseless subspace guarantees that $\Phi_{\Gamma_{2D}(\gamma_1,\gamma_2)}$ is never antidegradable.

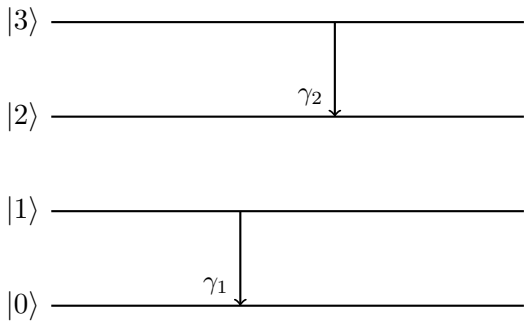

Figure 4.7.5: Class 2D is comprised of PCDS channels whose subchannels are ADC's

4.7.f Class 3A

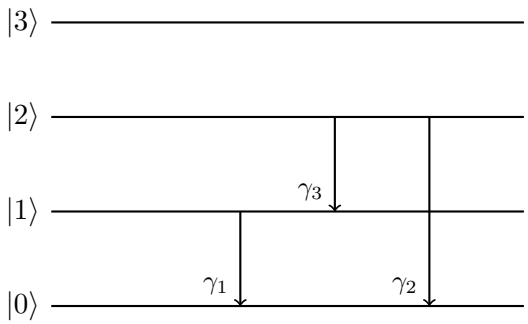

Figure 4.7.6: Class 3A consists of 3-dimensional MAD channels embedded into the higher dimensional $\mathcal{H}_4$

This class of channels consists PCDS channels whose subchannels are the identity channel $\Phi_{\mathrm{BB}} = \mathbb{1}_{\sigma(\mathcal{H}_1)}$ and a 3-dimensional MAD channel $\Phi_{\mathrm{AA}} = \Phi^{(3)}_{\Gamma(\gamma_1,\gamma_2,\gamma_3)}$. Turning off one of the decays reduces this class to one of the 2-decay classes:

- $\gamma_1 = 0 \Rightarrow$ Class 3A $\sim$ Class 2B
- $\gamma_2 = 0 \Rightarrow$ Class 3A $\sim$ Class 2C
- $\gamma_3 = 0 \Rightarrow$ Class 3A $\sim$ Class 2A

Let a generic channel belonging to this class be called $\Phi_{\Gamma_{3\mathrm{A}}(\gamma_1,\gamma_2,\gamma_3)}$; following (3.2.2) and (3.3.57), $\Phi^{(3)}_{\Gamma(\gamma_1,\gamma_2,\gamma_3)}$ is never degradable if $\gamma_1, \gamma_2, \gamma_3 \neq 0$. This also implies, as a consequence of (4.4.2), that it is not possible to build a 4-decay degradable MAD channel starting from a MAD channel belonging to Class 3A. The existence of a noiseless subspace guarantees that $\Phi_{\Gamma_{3\mathrm{A}}(\gamma_1,\gamma_2,\gamma_3)}$ is never antidegradable.

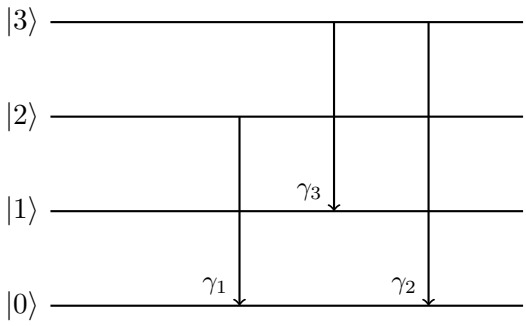

Figure 4.7.7: Class 3B

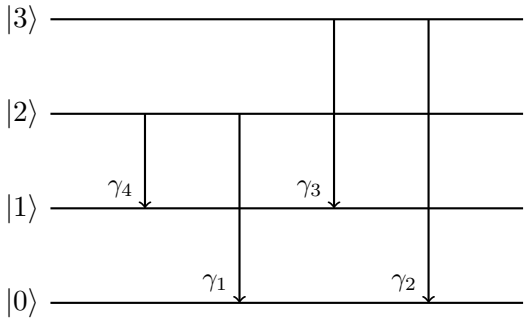

Figure 4.7.8: Class 4A

4.7.g Class 3B

Consider the transition matrix:

$$\Gamma_{3B}(\gamma_1,\gamma_2,\gamma_3) = \mathbb{1}_{\mathcal{H}_4} + \gamma_1 |2\rangle\langle 0| + \gamma_2 |3\rangle\langle 0| + \gamma_3 |3\rangle\langle 1| - \gamma_1 |2\rangle\langle 2| - (\gamma_2+\gamma_3) |3\rangle\langle 3|\,; \quad (4.7.6)$$

Class 3B is comprised of all the channels unitarily equivalent to $\Phi_{\Gamma_{3B}(\gamma_1,\gamma_2,\gamma_3)}$, depicted in Figure 4.7.7. Turning off one of the decays reduces this class to one of the 2-decay classes:

- $\gamma_1 = 0 \Rightarrow$ Class 3A $\sim$ Class 2B
- $\gamma_2 = 0 \Rightarrow$ Class 3A $\sim$ Class 2D
- $\gamma_3 = 0 \Rightarrow$ Class 3A $\sim$ Class 2A

The degradability conditions for this channel are:

$$\Phi_{\Gamma_{3B}(\gamma_1,\gamma_2,\gamma_3)} \text{ degradable} \Leftrightarrow \gamma_1 \leq \frac{1}{2} \wedge \gamma_2 + \gamma_3 \leq \frac{1}{2} \quad (4.7.7)$$

Starting from a channel in Class 3B, it is possible to build a degradable 4-decay MAD channel: consider the transition matrix:

$$\Gamma_{4A}(\gamma_1,\gamma_2,\gamma_3,\gamma_4) \equiv \Gamma_{3B}(\gamma_1,\gamma_2,\gamma_3) + \gamma_4 |2\rangle\langle 1| - \gamma_4 |2\rangle\langle 2| \quad (4.7.8)$$

The degradability conditions for $\Phi_{\Gamma_{4A}(\gamma_1,\gamma_2,\gamma_3,\gamma_4)}$ are:

$$\Phi_{\Gamma_{4A}(\gamma_1,\gamma_2,\gamma_3,\gamma_4)} \text{ degradable} \Leftrightarrow \gamma_1+\gamma_4 \leq \frac{1}{2} \wedge \gamma_2+\gamma_3 \leq \frac{1}{2} \tag{4.7.9}$$

This channel provides a counterexample to (4.7.1), proving that the relation is not a necessary condition for the degradability of a channel. The existence of a noiseless subspace for $\Phi_{\Gamma_{3B}(\gamma_1,\gamma_2,\gamma_3)}$ guarantees that the channel is never antidegradable.

4.7.h Class 3C

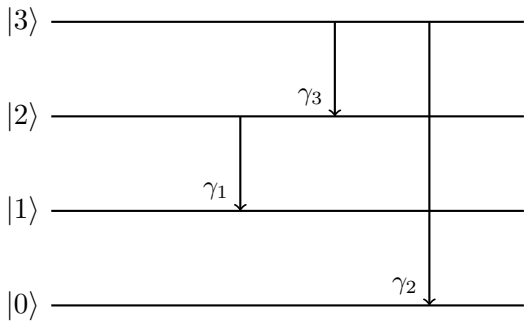

Figure 4.7.9: Class 3C

Consider the transition matrix:

$$\Gamma_{3C}(\gamma_1,\gamma_2,\gamma_3) = \mathbb{1}_{\mathcal{H}_4} + \gamma_1 |2\rangle\langle 1| + \gamma_2 |3\rangle\langle 0| + \gamma_3 |3\rangle\langle 2| - \gamma_1 |2\rangle\langle 2| - (\gamma_2+\gamma_3) |3\rangle\langle 3|\,; \tag{4.7.10}$$

Class 3C is comprised of all the channels unitarily equivalent to $\Phi_{\Gamma_{3C}(\gamma_1,\gamma_2,\gamma_3)}$, depicted in Figure 4.7.9. Turning off one of the decays reduces this class to one of the 2-decay classes:

- $\gamma_1 = 0 \Rightarrow$ Class 3C $\sim$ Class 2B
- $\gamma_2 = 0 \Rightarrow$ Class 3C $\sim$ Class 2C
- $\gamma_3 = 0 \Rightarrow$ Class 3C $\sim$ Class 2D

$\Phi_{\Gamma_{3C}(\gamma_1,\gamma_2,\gamma_3)}$ is never degradable when $\gamma_1,\gamma_2,\gamma_3 \neq 0$. The existence of a noiseless subspace guarantees that $\Phi_{\Gamma_{3C}(\gamma_1,\gamma_2,\gamma_3)}$ is never antidegradable.

4.7.i Class 3D

Consider the transition matrix:

$$\Gamma_{3D}(\gamma_1,\gamma_2,\gamma_3) = \mathbb{1}_{\mathcal{H}_4} + \gamma_1 |1\rangle\langle 0| + \gamma_2 |2\rangle\langle 1| + \gamma_3 |3\rangle\langle 0| - \gamma_1 |1\rangle\langle 1| - \gamma_2 |2\rangle\langle 2| - \gamma_3 |3\rangle\langle 3|\,; \tag{4.7.11}$$

Class 3D is comprised of all the channels unitarily equivalent to $\Phi_{\Gamma_{3D}(\gamma_1,\gamma_2,\gamma_3)}$, depicted in Figure 4.7.10. Turning off one of the decays reduces this class to one of the 2-decay classes:

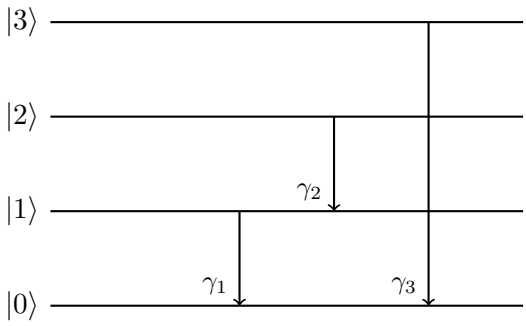

Figure 4.7.10: Class 3D

- $\gamma_1 = 0 \Rightarrow$ Class 3D $\sim$ Class 2D
- $\gamma_2 = 0 \Rightarrow$ Class 3D $\sim$ Class 2A
- $\gamma_3 = 0 \Rightarrow$ Class 3D $\sim$ Class 2C

$\Phi_{\Gamma_{3D}(\gamma_1,\gamma_2,\gamma_3)}$ is never degradable when $\gamma_1, \gamma_2, \gamma_3 \neq 0$.

4.7.j Class 3E

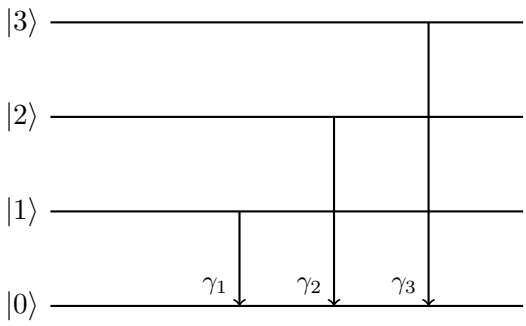

Figure 4.7.11: Class 3E

Consider the transition matrix:

$$\Gamma_{3E}(\gamma_1,\gamma_2,\gamma_3) = \mathbb{1}_{\mathcal{H}_4} + \gamma_1 |1\rangle\langle 0| + \gamma_2 |2\rangle\langle 0| + \gamma_3 |3\rangle\langle 0| - \gamma_1 |1\rangle\langle 1| - \gamma_2 |2\rangle\langle 2| - \gamma_3 |3\rangle\langle 3|\,; \quad (4.7.12)$$

Class 3D is comprised of all the channels unitarily equivalent to $\Phi_{\Gamma_{3E}(\gamma_1,\gamma_2,\gamma_3)}$, depicted in Figure 4.7.11. Turning off one of the decays reduces this class to one of the 2-decay classes:

- $\gamma_1 = 0 \Rightarrow$ Class 3E $\sim$ Class 2A
- $\gamma_2 = 0 \Rightarrow$ Class 3E $\sim$ Class 2A

- $\gamma_3 = 0 \Rightarrow$ Class 3E $\sim$ Class 2A

The degradability conditions for $\Phi_{\Gamma_{3E}(\gamma_1,\gamma_2,\gamma_3)}$ are:

$$\Phi_{\Gamma_{3E}(\gamma_1,\gamma_2,\gamma_3)} \text{ degradable} \Leftrightarrow \gamma_1 \leq \frac{1}{2} \wedge \gamma_2 \leq \frac{1}{2} \wedge \gamma_3 \leq \frac{1}{2} \tag{4.7.13}$$

4.7.k Class 3F

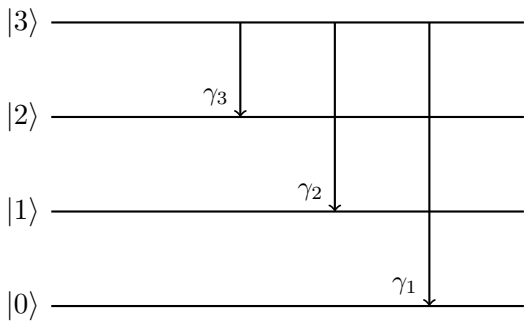

Figure 4.7.12: Class 3F

Consider the transition matrix:

$$\Gamma_{3E}(\gamma_1,\gamma_2,\gamma_3) = \mathbb{1}_{\mathcal{H}_4} + \gamma_1 |3\rangle\langle 0| + \gamma_2 |3\rangle\langle 1| + \gamma_3 |3\rangle\langle 2| - (\gamma_1+\gamma_2+\gamma_3) |3\rangle\langle 3|\,; \tag{4.7.14}$$

Class 3F is comprised of all the channels unitarily equivalent to $\Phi_{\Gamma_{3F}(\gamma_1,\gamma_2,\gamma_3)}$, depicted in Figure 4.7.12. Turning off one of the decays reduces this class to one of the 2-decay classes:

- $\gamma_1 = 0 \Rightarrow$ Class 3F $\sim$ Class 2B
- $\gamma_2 = 0 \Rightarrow$ Class 3F $\sim$ Class 2B
- $\gamma_3 = 0 \Rightarrow$ Class 3F $\sim$ Class 2B

The degradability conditions for $\Phi_{\Gamma_{3F}(\gamma_1,\gamma_2,\gamma_3)}$ are:

$$\Phi_{\Gamma_{3F}(\gamma_1,\gamma_2,\gamma_3)} \text{ degradable} \Leftrightarrow \gamma_1 \leq \frac{1}{2} \wedge \gamma_2 \leq \frac{1}{2} \wedge \gamma_3 \leq \frac{1}{2} \tag{4.7.15}$$

The existence of a noiseless subspace guarantees that $\Phi_{\Gamma_{3F}(\gamma_1,\gamma_2,\gamma_3)}$ is never antidegradable.

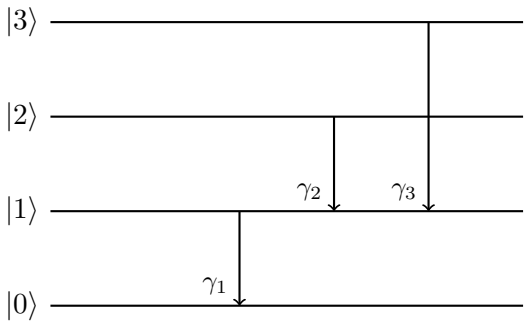

Figure 4.7.13: Class 3G

4.7.l Class 3G

Consider the transition matrix:

$$\Gamma_{3G}(\gamma_1,\gamma_2,\gamma_3) = \mathbb{1}_{\mathcal{H}_4} + \gamma_1 |1\rangle\langle 0| + \gamma_2 |2\rangle\langle 1| + \gamma_3 |3\rangle\langle 1| - \gamma_1 |1\rangle\langle 1| - \gamma_2 |2\rangle\langle 2| - \gamma_3 |3\rangle\langle 3|\,; \quad (4.7.16)$$

Class 3G is comprised of all the channels unitarily equivalent to $\Phi_{\Gamma_{3G}(\gamma_1,\gamma_2,\gamma_3)}$, depicted in Figure 4.7.13. Turning off one of the decays reduces this class to one of the 2-decay classes:

- $\gamma_1 = 0 \Rightarrow$ Class 3G $\sim$ Class 2A
- $\gamma_2 = 0 \Rightarrow$ Class 3G $\sim$ Class 2C
- $\gamma_3 = 0 \Rightarrow$ Class 3G $\sim$ Class 2C

$\Phi_{\Gamma_{3G}(\gamma_1,\gamma_2,\gamma_3)}$ is never degradable when $\gamma_1, \gamma_2, \gamma_3 \neq 0$.

4.7.m Class 3H

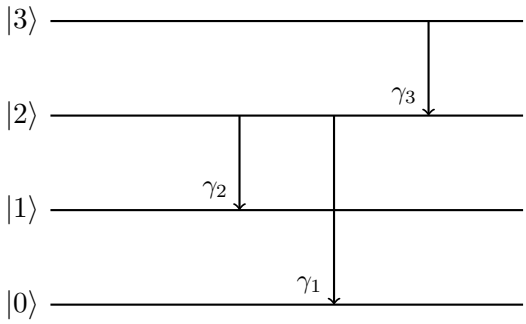

Figure 4.7.14: Class 3H

Consider the transition matrix:

$$\Gamma_{3H}(\gamma_1,\gamma_2,\gamma_3) = \mathbb{1}_{\mathcal{H}_4} + \gamma_1 |2\rangle\langle 0| + \gamma_2 |2\rangle\langle 1| + \gamma_3 |3\rangle\langle 2| - (\gamma_1+\gamma_2) |2\rangle\langle 2| - \gamma_3 |3\rangle\langle 3|\,; \quad (4.7.17)$$

Class 3H is comprised of all the channels unitarily equivalent to $\Phi_{\Gamma_{3H}(\gamma_1,\gamma_2,\gamma_3)}$, depicted in Figure 4.7.14. Turning off one of the decays reduces this class to one of the 2-decay classes:

- $\gamma_1 = 0 \Rightarrow$ Class 3H $\sim$ Class 2C
- $\gamma_2 = 0 \Rightarrow$ Class 3H $\sim$ Class 2C
- $\gamma_3 = 0 \Rightarrow$ Class 3H $\sim$ Class 2B

$\Phi_{\Gamma_{3H}(\gamma_1,\gamma_2,\gamma_3)}$ is never degradable when $\gamma_1, \gamma_2, \gamma_3 \neq 0$.

4.7.n Class 3I

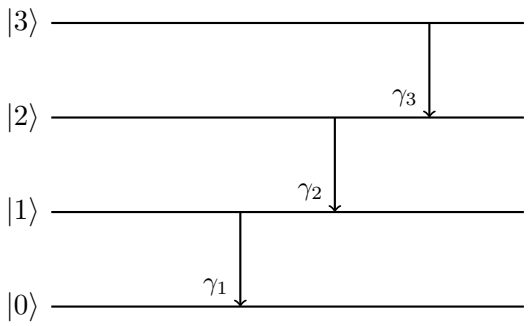

Figure 4.7.15: Class 3I

Consider the transition matrix:

$$\Gamma_{3I}(\gamma_1,\gamma_2,\gamma_3) = \mathbb{1}_{\mathcal{H}_4} + \gamma_1 |1\rangle\langle 0| + \gamma_2 |2\rangle\langle 1| + \gamma_3 |3\rangle\langle 2| - \gamma_1 |1\rangle\langle 1| - \gamma_2 |2\rangle\langle 2| - \gamma_3 |3\rangle\langle 3|\,; \quad (4.7.18)$$

Class 3I is comprised of all the channels unitarily equivalent to $\Phi_{\Gamma_{3I}(\gamma_1,\gamma_2,\gamma_3)}$, depicted in Figure 4.7.15. Turning off one of the decays reduces this class to one of the 2-decay classes:

- $\gamma_1 = 0 \Rightarrow$ Class 3I $\sim$ Class 2C
- $\gamma_2 = 0 \Rightarrow$ Class 3I $\sim$ Class 2D
- $\gamma_3 = 0 \Rightarrow$ Class 3I $\sim$ Class 2C

$\Phi_{\Gamma_{3I}(\gamma_1,\gamma_2,\gamma_3)}$ is never degradable when $\gamma_1, \gamma_2, \gamma_3 \neq 0$.

4.8 Antidegradability of MAD channels

The reasoning behind 4.6 could be repeated here if one knew how to build the right inverse of the complementary channel $\tilde{\Phi}_\Gamma$. In fact, the region of antidegradability of $\tilde{\Phi}_\Gamma$ corresponds to the region where $\tilde{\Lambda}_\Gamma$:

$$\tilde{\Lambda}_\Gamma \equiv \Phi \circ \tilde{\Phi}_\Gamma^{(-1)} \tag{4.8.1}$$

is completely positive. However, there is an easier way to find that region.

The composition of antidegradable channels is antidegradable; this means that, given the composition in (4.2.11), a sufficient condition for the antidegradability of Φ_Γ is the antidegradability of all Φ_{Γ_i}'s:

$$\Phi_{\Gamma_i} \text{ antidegradable } \forall 1 \leq i \leq d-1 \Rightarrow \Phi_\Gamma \text{ antidegradable} \tag{4.8.2}$$

TODO encode in subspace bla bla.

$$\Phi_{\Gamma_i} \text{ antidegradable } \forall 1 \leq i \leq d-1 \Leftrightarrow \Phi_\Gamma \text{ antidegradable} \tag{4.8.3}$$

4.9 Degradability of a MAD channel embedded in a higher dimensional system

TODO The structure defined in (3.2.1) lends itself very well to the case of MAD channels; in fact, given a d-dimensional MAD channel $\Phi_\Gamma : \sigma(\mathcal{H}_d) \mapsto \sigma(\mathcal{H}_d)$, one may consider another MAD channel $\Phi_{\bar{\Gamma}} : \sigma(\mathcal{H}_{d+1}) \mapsto \sigma(\mathcal{H}_{d+1})$ whose transition probabilities are:

$$\bar{\gamma}_{ji} = \begin{cases} \gamma_{ji} & \text{if } 0 \leq i < j \leq d-1 \\ 0 & \text{if } 0 \leq i < j = d \end{cases} \tag{4.9.1}$$

In the context of (3.2.1), the Φ_{AA} and Φ_{BB} channels of $\Phi_{\bar{\Gamma}}$ are Φ_Γ and $\mathbb{1}_{\mathcal{H}_1}$. Then, (3.2.2) implies that $\Phi_{\bar{\Gamma}}$ is degradable if and only if Φ_Γ is degradable.

4.10 Monotonicity properties

In [CG21a], using the pipeline inequalities **??** and the monotonicity of the 3-dimensional MAD channels in their parameters, proven in 3.3.g, the authors were able to compute some capacity functionals for certain configurations of the channels that were not degradable nor anti-degradable. In order to generalize the property of monotonicity of the capacity functionals to the d-dimensional case, one needs to consider two transition matrices, Γ, Γ', whose elements $\gamma_{ji}, \gamma'_{ji}$ differ only for a single pair of indices (j_0, i_0), so that:

$$\gamma'_{j_0,i_0} \geq \gamma_{j_0,i_0}. \tag{4.10.1}$$

Then, on account of the pipeline inequalities **??**, one could conclude that the capacities MAD channels are non increasing in the parameter $\gamma'_{j_0,i_0} \geq \gamma_{j_0,i_0}$ if one were able to find two LCPT maps Λ_L, Λ_R such that:

$$\Lambda_L \circ \Phi_\Gamma \circ \Lambda_R = \Phi_{\Gamma'} \tag{4.10.2}$$

Finding Λ_L, Λ_R is not an easy task and generally one has to resort to heuristic methods to simplify the problem. Recalling the property of closure under composition for MAD channels, one might assume that Λ_L, Λ_R are MAD's themselves; however, for $d > 3$, this line of reasoning only allows to derive monotonicity properties under the transition probabilities γ_{d-1,i_0}, $\forall\ 0 \leq i_0 < d-1$ and γ_{10}:

- **Monotonicity under** γ_{d-1,i_0}: Consider $\Lambda_R = \mathbb{1}_{\mathcal{H}_d}$ the identity channel and $\Lambda_L = \Phi_{\Gamma_{\lambda_{d-1,i_0}}}$ a single decay MAD channel from $|d-1\rangle$ to $|i_0\rangle$ with transition probability λ_{d-1,i_0}. From (4.2.7), the resulting channel in (4.10.2), $\Phi_{\Gamma'} = \Phi_{\Gamma_{\lambda_{d-1,i_0}}} \circ \Phi_\Gamma$ has the same transition probabilities γ'_{ji} of Φ_Γ aside from $\gamma'_{d-1,i_0} \geq \gamma_{d-1,i_0}$

- **Monotonicity under** γ_{10}: Consider $\Lambda_L = \mathbb{1}_{\mathcal{H}_d}$ the identity channel and $\Lambda_R = \Phi_{\Gamma_{\lambda_{10}}}$ a single decay MAD channel from $|1\rangle$ to $|0\rangle$ with transition probability λ_{10}. From (4.2.7), the resulting channel in (4.10.2), $\Phi_{\Gamma'} = \Phi_\Gamma \circ \Phi_{\Gamma_{\lambda_{10}}}$ has the same transition probabilities γ'_{ji} of Φ_Γ aside from $\gamma'_{10} \geq \gamma_{10}$

Monotonicity properties in $d = 4$

It is unclear whether a 4-dimensional MAD channel presents monotonous capacities under the transition probabilities γ_{20}, γ_{21}. As stated above, resorting to (4.10.2) is only useful if additional assumptions are made. Assume that either one of $\Lambda_L, \Lambda_R = \mathbb{1}_{\mathcal{H}_d}$, then, utilizing the inverse map (4.5.7), from (4.10.2):

$$\Lambda_R = \mathbb{1}_{\mathcal{H}_d} \Rightarrow \Lambda_L = \Phi_{\Gamma'} \circ \Phi_\Gamma^{(-1)} \tag{4.10.3}$$

$$\Lambda_L = \mathbb{1}_{\mathcal{H}_d} \Rightarrow \Lambda_R = \Phi_\Gamma^{(-1)} \circ \Phi_{\Gamma'} \tag{4.10.4}$$

Note that, by construction, both of these maps are linear and trace preserving; verifying their complete positiveness would imply that they are quantum channels, which can be done by verifying the positive semi-definiteness of their Choi matrices, due to (**??**).

$\gamma'_{21} \geq \gamma_{21}$

Assume that Γ' and Γ only differ in the $|2\rangle\langle 1|$ element, so that:

$$\begin{gathered} \gamma'_{21} \equiv \gamma_{21} + \varepsilon_{21} \geq \gamma_{21} \\ 0 \leq \varepsilon_{21} \leq \gamma_{22} \end{gathered} \tag{4.10.5}$$

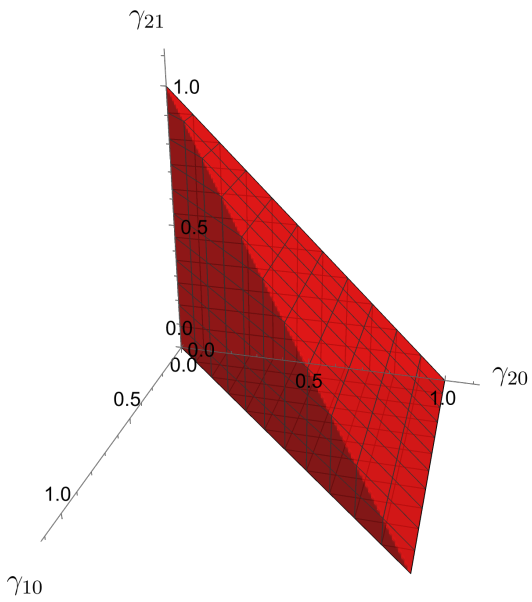

Figure 4.10.1: Monotonicity region under γ_{21} (4.10.7). Note that γ_{21}, γ_{20} are still bounded by (3.3.3), meaning that $0 \leq \gamma_{20} + \gamma_{21} \leq 1$.

where the last condition is needed in order for $\gamma_{22'} = \gamma_{22} - \varepsilon_{21} \geq 0$ to be satisfied. Computing the eigenvalues of the Choi matrices of Λ_L, Λ_R in (4.10.3) and (4.10.4), one finds that the former is only positive semi-definite if:

$$\gamma_{32} = 0, \tag{4.10.6}$$

while the latter is positive semi-definite under the following condition:

$$\gamma_{20} - \gamma_{10} \geq 0 \tag{4.10.7}$$

which means that the capacity functionals of a 4-dimensional MAD channel are monotonous under γ_{21} if $\gamma_{32} = 0$ or $\gamma_{20} \geq \gamma_{10}$. The region described by (4.10.7) is illustrated in Figure 4.10.1.

$\gamma'_{20} \geq \gamma_{20}$

Assume that Γ' and Γ only differ in the $|2\rangle\langle 0|$ element, so that:

$$\begin{gathered} \gamma'_{20} \equiv \gamma_{20} + \varepsilon_{20} \geq \gamma_{20} \\ 0 \leq \varepsilon_{20} \leq \gamma_{22} \end{gathered} \tag{4.10.8}$$

where the last condition is needed in order for $\gamma_{22'} = \gamma_{22} - \varepsilon_{20} \geq 0$ to be satisfied. Computing the eigenvalues of the Choi matrices of Λ_L, Λ_R in (4.10.3) and (4.10.4), one finds that the former is only positive semi-definite if:

$$\gamma_{32} = 0, \tag{4.10.9}$$

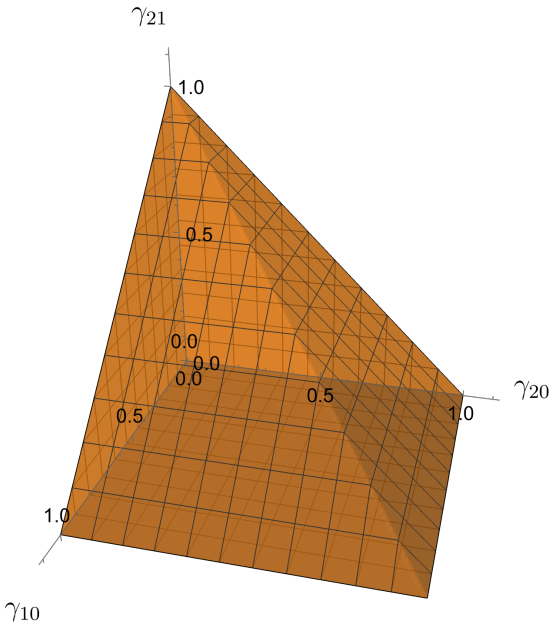

Figure 4.10.2: Monotonicity region under γ_{20} (4.10.10). Note that γ_{21}, γ_{20} are still bounded by (3.3.3), meaning that $0 \leq \gamma_{20} + \gamma_{21} \leq 1$.

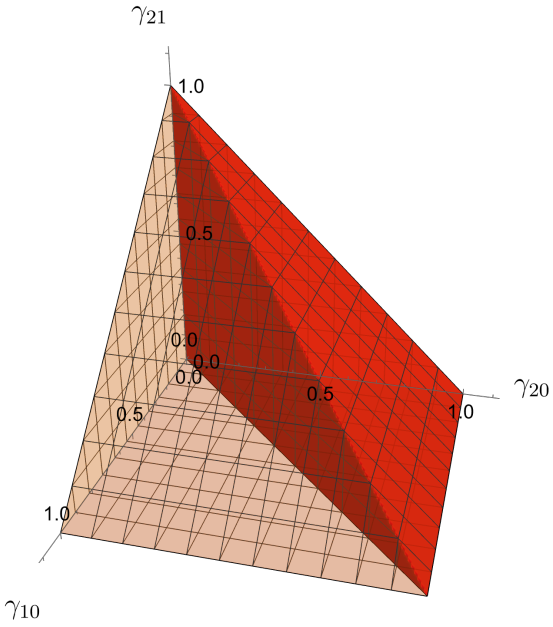

Figure 4.10.3: The monotonicity region under γ_{21} (4.10.7) is completely contained within the monotonicity region under γ_{20} (4.10.10).

while the latter is positive semi-definite under the following condition:

$$1 - \gamma_{21} - \gamma_{10} \geq 0 \tag{4.10.10}$$

which means that the capacity functionals of a 4-dimensional MAD channel are monotonous under γ_{20} if $\gamma_{32} = 0$ or $\gamma_{21} \leq 1 - \gamma_{10}$. The region described by (4.10.10) is illustrated in Figure 4.10.2. Note that the region described by (4.10.7) is completely contained within the region described by (4.10.10), as can be seen in Figure 4.10.3, meaning that if the capacity functionals of a 4-dimensional MAD channel are monotonous under the parameter γ_{21}, then they are also monotonous under the parameter γ_{20}.

5

Capacitiy computations for MAD channels in $d = 4$

Building upon the results in Chapters 2, 3 and 4, applying the techniques described in **??**, an analysis of the quantum, private classical and two-way capacities 4-dimensional MAD channel becomes feasible. This analysis was performed and the consequent results are reported in this chapter.

5.1 Section 1

6
Conclusion

Lorem ipsum dolor sit amet, consectetuer adipiscing elit. Ut purus elit, vestibulum ut, placerat ac, adipiscing vitae, felis. Curabitur dictum gravida mauris. Nam arcu libero, nonummy eget, consectetuer id, vulputate a, magna. Donec vehicula augue eu neque. Pellentesque habitant morbi tristique senectus et netus et malesuada fames ac turpis egestas. Mauris ut leo. Cras viverra metus rhoncus sem. Nulla et lectus vestibulum urna fringilla ultrices. Phasellus eu tellus sit amet tortor gravida placerat. Integer sapien est, iaculis in, pretium quis, viverra ac, nunc. Praesent eget sem vel leo ultrices bibendum. Aenean faucibus. Morbi dolor nulla, malesuada eu, pulvinar at, mollis ac, nulla. Curabitur auctor semper nulla. Donec varius orci eget risus. Duis nibh mi, congue eu, accumsan eleifend, sagittis quis, diam. Duis eget orci sit amet orci dignissim rutrum.

Nam dui ligula, fringilla a, euismod sodales, sollicitudin vel, wisi. Morbi auctor lorem non justo. Nam lacus libero, pretium at, lobortis vitae, ultricies et, tellus. Donec aliquet, tortor sed accumsan bibendum, erat ligula aliquet magna, vitae ornare odio metus a mi. Morbi ac orci et nisl hendrerit mollis. Suspendisse ut massa. Cras nec ante. Pellentesque a nulla. Cum sociis natoque penatibus et magnis dis parturient montes, nascetur ridiculus mus. Aliquam tincidunt urna. Nulla ullamcorper vestibulum turpis. Pellentesque cursus luctus mauris.

Nulla malesuada porttitor diam. Donec felis erat, congue non, volutpat at, tincidunt tristique, libero. Vivamus viverra fermentum felis. Donec nonummy pellentesque ante. Phasellus adipiscing semper elit. Proin fermentum massa ac quam. Sed diam turpis, molestie vitae, placerat a, molestie nec, leo. Maecenas lacinia. Nam ipsum ligula, eleifend at, accumsan nec, suscipit a, ipsum. Morbi blandit ligula feugiat magna. Nunc eleifend consequat lorem. Sed lacinia nulla vitae enim. Pellentesque tincidunt purus vel magna. Integer non enim. Praesent euismod nunc eu purus. Donec bibendum quam in tellus. Nullam cursus pulvinar lectus. Donec et mi. Nam vulputate metus eu enim. Vestibulum pellentesque felis eu massa.

Acknowledgement

First, I like to thank my daily supervisor ..., for there support. Also, I wan to thank my first supervisor ... for his insight into.
Thanks to ..... for all the insights into .... . Thanks to .... for all the intense but fruitful scientific debate about .... . Thanks to ... , who always had an open door for ..... .
Also, I would like to thank the .... .
And last but not least, thanks to .... , who helped ..... . As well as .... for the help with .... .

Bibliography

[Bel64] J. S. Bell. On the Einstein Podolsky Rosen paradox. *Physics Physique Fizika*, 1:195–200, November 1964.

[CG21a] Stefano Chessa and Vittorio Giovannetti. Quantum capacity analysis of multi-level amplitude damping channels. *Communications Physics*, 4(1):22, February 2021.

[CG21b] Stefano Chessa and Vittorio Giovannetti. Partially Coherent Direct Sum Channels. *Quantum*, 5:504, July 2021.

[Cho75] Man-Duen Choi. Completely positive linear maps on complex matrices. *Linear Algebra and its Applications*, 10(3):285–290, 1975.

[Dys49] F. J. Dyson. The Radiation Theories of Tomonaga, Schwinger, and Feynman. *Phys. Rev.*, 75:486–502, February 1949.

[GF05] Vittorio Giovannetti and Rosario Fazio. Information-capacity description of spin-chain correlations. *Phys. Rev. A*, 71:032314, March 2005.

[Gor62] J. P. Gordon. Quantum Effects in Communications Systems. *Proceedings of the IRE*, 50(9):1898–1908, 1962.

[Hol07] A.S. Holevo. Complementary Channels and the Additivity Problem. *Theory of Probability & Its Applications*, 51(1):92–100, 2007.

[Hol13] Alexander S. Holevo. *Quantum Systems, Channels, Information*. De Gruyter, 2013.

[Jam72] A. Jamiołkowski. Linear transformations which preserve trace and positive semidefiniteness of operators. *Reports on Mathematical Physics*, 3(4):275–278, 1972.

[NC10] Michael A. Nielsen and Isaac L. Chuang. *Quantum Computation and Quantum Information: 10th Anniversary Edition*. Cambridge University Press, 2010.

[Sha48] C. E. Shannon. A mathematical theory of communication. *The Bell System Technical Journal*, 27(3):379–423, 1948.

[Sti55] W. Forrest Stinespring. Positive Functions on C*-Algebras. *Proceedings of the American Mathematical Society*, 6(2):211–216, 1955.

Appendix

Big Matrices

$$
\begin{pmatrix}
\gamma_{10}\rho_{00} + (1-\gamma_{10})\rho_{11} + (1-\gamma_{20}-\gamma_{21})\rho_{22} + (1-\gamma_{30}-\gamma_{31}-\gamma_{32})\rho_{33} & \sqrt{\gamma_{10}}\rho_{01} & \sqrt{\gamma_{20}}\rho_{02} & \sqrt{1-\gamma_{10}}\sqrt{\gamma_{21}}\rho_{12} & \sqrt{\gamma_{30}}\rho_{03} & \sqrt{1-\gamma_{10}}\sqrt{\gamma_{31}}\rho_{13} & \sqrt{1-\gamma_{20}-\gamma_{21}}\sqrt{\gamma_{32}}\rho_{23} \\
(\rho_{01})^{*}\sqrt{\gamma_{10}} & \gamma_{10}\rho_{11} & \sqrt{\gamma_{10}}\sqrt{\gamma_{20}}\rho_{12} & 0 & \sqrt{\gamma_{10}}\sqrt{\gamma_{30}}\rho_{13} & 0 & 0 \\
(\rho_{02})^{*}\sqrt{\gamma_{20}} & (\rho_{12})^{*}\sqrt{\gamma_{10}}\sqrt{\gamma_{20}} & \gamma_{20}\rho_{22} & \gamma_{21}\rho_{22} & \sqrt{\gamma_{20}}\sqrt{\gamma_{30}}\rho_{23} & \sqrt{\gamma_{21}}\sqrt{\gamma_{31}}\rho_{23} & 0 \\
(\rho_{12})^{*}\sqrt{1-\gamma_{10}}\sqrt{\gamma_{21}} & 0 & 0 & 0 & 0 & 0 & 0 \\
(\rho_{03})^{*}\sqrt{\gamma_{30}} & (\rho_{13})^{*}\sqrt{\gamma_{10}}\sqrt{\gamma_{30}} & (\rho_{23})^{*}\sqrt{\gamma_{20}}\sqrt{\gamma_{30}} & 0 & \gamma_{30}\rho_{33} & \gamma_{31}\rho_{33} & 0 \\
(\rho_{13})^{*}\sqrt{1-\gamma_{10}}\sqrt{\gamma_{31}} & 0 & 0 & (\rho_{23})^{*}\sqrt{\gamma_{21}}\sqrt{\gamma_{31}} & 0 & 0 & \gamma_{32}\rho_{33} \\
(\rho_{23})^{*}\sqrt{1-\gamma_{20}-\gamma_{21}}\sqrt{\gamma_{32}} & 0 & 0 & 0 & 0 & 0 & 0
\end{pmatrix}
\tag{9.1}
$$

Proofs

Computation methods